TAMPEREEN TEKNILLINEN YLIOPISTO
TAMPERE UNIVERSITY OF TECHNOLOGY
Julkaisu 849 • Publication 849

Satu Kärki

Film-type Sensor Materials in Measurement of Physiological Force and Pressure Variables

Tampere 2009

Tampereen teknillinen yliopisto. Julkaisu 849
Tampere University of Technology. Publication 849

Satu Kärki

Film-type Sensor Materials in Measurement of Physiological Force and Pressure Variables

Thesis for the degree of Doctor of Technology to be presented with due permission for public examination and criticism in Sähkötalo Building, Auditorium S2, at Tampere University of Technology, on the 20th of November 2009, at 12 noon.

Tampereen teknillinen yliopisto - Tampere University of Technology
Tampere 2009

ISBN 978-952-15-2265-9 (printed)
ISBN 978-952-15-2313-7 (PDF)
ISSN 1459-2045

Abstract

Measurement of physiological signals reveals valuable information on the physiological state of a patient. In this thesis, new and unobtrusive ways to measure physiological force and pressure variables with film-type sensor materials are explored. The measured variables are divided into two application areas; the first is related to cardiopulmonary variables while the second one is concentrated on plantar pressure mapping. In the area of cardiopulmonary variables, the measurement of heart and respiration rates and heart sounds are studied. Pressure mapping, instead, provides information on the interface pressure distribution between a person and the surface the person is on. Here the plantar pressure distribution between a foot and ground or shoe is measured to find out regions of the plantar area where the pressure has high values. The high pressure values are linked with pressure ulcers.

Two film-type sensor materials are used here; polyvinylidenefluoride (PVDF) and ElectroMechanical Film (EMFi). The semicrystalline PVDF material has solid structure whereas the structure of the EMFi material is cellular. However, both materials generate a charge when they are mechanically deformed and thus, in principle, operate similarly. With normal measurement arrangement, PVDF and EMFi are not suitable for static measurements and only the change of an external force can be measured. Hence, the sensors made of these materials are useful especially in the measurements of physiological pulsatile signals. The sensors used in this thesis are constructed manually from commercial film materials. The entire measurement process is considered; from the design and construction of the sensors and measurement devices to the analysis of the measured data with Matlab® software.

In the measurements of cardiopulmonary variables, the sensor attachments are minimized and the measurement systems are designed to be unobtrusive and comfortable for the user. The sensors utilizing the PVDF and/or EMFi materials can be integrated into clothing or into daily life objects (e.g. a chair or a bed) to measure vital signals. This thesis suggests that the both sensor materials are suitable for such measurements even though some differences between the results obtained with the materials were found. In the area of the plantar pressure measurements, instead, a new sensor prototype for pressure measurements during gait is introduced. The developed sensor utilizes commercial PVDF material with silver ink metallization and it simultaneously measures both normal and shear stresses. Also, a sensor based on unmetallized PVDF material with printed electrodes is tested. Based on the promising results obtained with these sensor prototypes, the aim is to further develop a matrix version of the sensor for on-floor and also in-shoe plantar pressure measurements.

Preface

The work presented in this thesis was carried out in the Department of Automation Science and Engineering at Tampere University of Technology (TUT), Finland, during the years 2004 – 2009.

First, I would like to express my gratitude to my supervisor Prof. Jukka Lekkala for his support and encouragement during this work. I also want to thank Prof. Jouko Halttunen, the head of the Department of Automation Science and Engineering, for his guidance. Special thanks go to M.D. Hannu Kuokkanen for the interesting application area he provided to my research. I also want to thank Ms. Tiina Kaistila, M.D. Minna Kääriäinen, M.D. Heikki-Jussi Laine and M.D. Heikki Mäenpää from Tampere University Hospital. Thanks are also for PhD Matti Mäntysalo from the Department of Electronics, TUT, for his help.

I am grateful to my colleagues in the Department of Automation Science and Engineering, especially to the members of the former Institute of Measurement and Information Technology. I thank PhD Heikki Jokinen and laboratory engineer Heimo Ihalainen for their valuable advices with the Matlab® software. I also want to thank the members of our sensor technology group. Especially I wish to thank M.Sc. Timo Salpavaara and M.Sc. Antti Vehkaoja.

I would like to thank the reviewers, Prof. Siegfried Bauer (Johannes Kepler University Linz, Austria) and Prof. Raimo Sepponen (Helsinki University of Technology, Finland), for their constructive comments.

The financial support of Finnish Cultural Foundation (Ulla and Eino Karosuo foundation) is gratefully acknowledged.

Finally, I want to express my sincere gratitude to my family and friends for their support during this process.

Tampere, November 2009

Satu Rämö

List of Acronyms

AD820	Operational amplifier, Analog Devices
AP	Anterior-posterior
BCG	Ballistocardiogram
BP	Bandpass
BSN	Body sensor network
ECG	Electrocardiogram
EMFi	ElectroMechanical Film
ETMF	Electro-thermo-mechanical film
LP	Lowpass
ML	Medial-lateral
NTC	Negative Temperature Coefficient
PCG	Phonocardiography
PP	Polypropylene
PSD	Power spectral density
PVDF	Polyvinylidenefluoride
P(VDF-TrFE)	Poly(vinylidenefluoride - trifluoroethylene)
RR	Respiration rate
S1	The first heart sound
S2	The second heart sound
S3	The third heart sound
S4	The fourth heart sound
SA	Sinoatrial
SCB-68	Connector block, National Instruments
SCSB	Static charge sensitive bed
SEM	Scanning electron microscope
TrFE	Trifluoroethylene
WSN	Wireless sensor network

List of Symbols

A	Area; gain
$A_{\max}$	Maximum passband variation
$A_k(n)$	Fourier transform; $k = 1, 2, \ldots, K$; $n = 0, \ldots, L/2$
C	Capacitor; capacitance
C_{f}	Feedback capacitor
C_s	Film capacitance
D	Electric flux density
d, d_{ij}, d_{3n}	Piezoelectric coefficient, unit C / N (direct effect)
e	Piezoelectric coefficient, unit C / m² (direct effect)
E	Electric field strength
e_{n}	Spectral density (voltage source)
ε	Permittivity
ε_0	Permittivity of vacuum
ϵ	Constant, determines the maximum passband variation A_{max}
f	Frequency
F	Force
$F_{\parallel}$	Force tangential to a material surface
ΔF	Impact force
g	Acceleration of free fall
g, g_{ij}, g_{3n}	Piezoelectric coefficient, unit Vm / N (direct effect)
h	Piezoelectric coefficient, unit V / m (direct effect)
$\lvert H(j\omega)\rvert$	Magnitude response
i	Imaginary number; $i = (-1)^{1/2}$
i_{n}	Spectral density (current source)
$I_k(f_n)$	Modified periodogram; $k = 1, 2, \ldots, K$
K	Number of segments
L	Length of segments
m	Mass
n	Order of the Butterworth filter; index for the Fourier transform components
p	Pressure; pyroelectric coefficient
$\hat{P}(f_n)$	Welch spectral estimate
Q	Charge
r	Overlap ratio
R	Resistor

R_s	Internal leak resistance
ρ	Mass density
s	Compliance
S	Strain
S_q	Sensitivity of an EMFi sensor
t	Film thickness
T_c	Glass transition temperature
τ	Time constant
U	Coefficient to remove the windowing effect from the total signal power
V_0	Output voltage of a PVDF sensor
V_{out}	Voltage output
ΔV	Output voltage of an EMFi sensor
$W(j)$	Data window; $j = 0, \dots, L-1$
X, X_n	Stress
$X(j)$	Segment; $j = 0, \dots, L-1$
Y	Young's modulus
ω	Angular frequency; $\omega = 2\pi f$
ω_c	Cut-off frequency

Contents

List of Publications

This thesis is based on the following publications. These publications are referred to in the text as Publication I, Publication II and so on.

I S. Kärki & J. Lekkala. Film-type transducer materials PVDF and EMFi in the measurement of heart and respiration rates. In *Proceedings of the 30th Annual International Conference of the IEEE Engineering in Medicine and Biology Society (EMBC 2008)*, 2008, Vancouver, British Columbia, Canada, p. 530-533.

II S. Kärki & J. Lekkala. A new method to measure heart rate with EMFi and PVDF materials. *Journal of Medical Engineering and Technology*, Vol. 33, No. 7, p. 551-558, Oct. 2009.

III S. Kärki, M. Kääriäinen & J. Lekkala. Measurement of heart sounds with EMFi transducer. In *Proceedings of the 29th Annual International Conference of the IEEE Engineering in Medicine and Biology Society (EMBC 2007)*, 2007, Lyon, France, p. 1683-1686.

IV S. Kärki, J. Lekkala, H. Kuokkanen & J. Halttunen. Development of a piezoelectric polymer film sensor for plantar normal and shear stress measurements. *Sensors and Actuators A: Physical*, Vol. 154, p. 57-64, Aug. 2009.

V S. Kärki, M. Kiiski, M. Mäntysalo & J. Lekkala. A PVDF sensor with printed electrodes for normal and shear stress measurements on sole. In *Proceedings of the IMEKO XIX World Congress*, 2009, Lisbon, Portugal, p. 1765-1769.

VI S. Kärki & J. Lekkala. Modeling sensor properties of PVDF and EMFi materials. *Measurement*, submitted.

The author of this thesis contributed to the publications as follows. In Publications I, II and III the author designed the study, implemented the transducers and measurement electronics, carried out the test measurements and data analysis and wrote the major parts of the manuscripts. In Publication III M.D. Minna Kääriäinen revised the physiological statements concerning the origin of heart sounds.

In Publication IV the author designed the study, implemented the sensor prototype and measurement electronics, carried out the test measurements and data analysis and wrote the major part of the manuscript. M.D. Hannu Kuokkanen and Prof. Jouko Halttunen revised the statements concerning the medical background of plantar stress measurements and

metrology, respectively. Publication V was jointly written by the author and PhD Matti Mäntysalo. M.Sc. Miika Kiiski implemented the sensor prototypes for the study and the author carried out the test measurements. In Publication VI, the model was jointly designed by the author and Prof. Jukka Lekkala. The author was also responsible for the test measurements and wrote the major part of the manuscript. Manuscripts for Publications I – VI were all revised by Prof. Jukka Lekkala.

Supplementary Publications

The following supplementary publications are not included into this thesis but they are closely related to its contents and therefore separated from the list of references.

VII S. Kärki & J. Lekkala. Pressure mapping system for physiological measurements. In *Proceedings of the IMEKO XVIII World Congress and IV Brazilian Congress of Metrology*, 2006, Rio de Janeiro, Brazil, 5 p.

VIII S. Kärki, M. Lehto & J. Lekkala. Painekartoitus painehaavojen ehkäisyn apuna. *Duodecim Medical Journal*, Vol. 122, p. 671-676, 2006 (in Finnish).

IX S. Kärki, J. Lekkala, T. Kaistila, H.-J. Laine, H. Mäenpää & H. Kuokkanen. Plantar pressure distribution measurements: An approach to different methods to compute a pressure map. In *Proceedings of the IMEKO XIX World Congress*, 2009, Lisbon, Portugal, p. 1770-1774.

Chapter 1

Introduction

The field of medical physics, also called as medical or biomedical engineering, overlaps two large fields of medicine and physics [14]. The field can be defined as "the use of the principles and techniques of engineering to solve problems in biology and medicine" [69]. The field is very wide, and it includes several subgroups such as medical imaging, computer analysis of the human genome, and medical instrumentation [69]. The field of this thesis concentrates on the last; however, also measurement and sensor technologies are considered. New ways to measure physiological force and pressure variables with film-type sensor materials are explored. In this thesis two materials are applied, polyvinylidenefluoride (PVDF) and ElectroMechanical Film (EMFi). Force and pressure are closely related to each other and thus similar sensor solutions can be used to measure both quantities.

The physiological force and pressure variables are divided here into two application areas. The first is related to cardiopulmonary variables. The term cardiopulmonary refers to heart and lungs and their functions [116] and the variables discussed here are heart rate, respiration and heart sounds. Several devices measuring these variables have been developed during the last few decades. For example, PVDF has been utilized in the measurement of respiration and cardiac action [19], [20], [96]. Similar measurements are also done with the EMFi material [1], [51], [52], [55], [81], [87], [97].

Measurement of vital signals, such as heart rate and respiration, reveals valuable information on the physiological state of the patient. Diseases such as sleep apnea syndrome and sudden infant death syndrome usually happen during sleep and are thus difficult to detect without continuous monitoring [19], [20]. Also, due to the increasing age of people in society, the need of monitoring devices to measure the vital signals at home is growing [70]. However, there have been relatively few methods to record these variables without direct contact between an electrode and skin [96] until now. Nowadays, new sensor materials offer a possibility to monitor vital signals unobtrusively. Thin sensors implemented from these materials can be easily integrated into clothing ("wearable") or into daily life objects, e.g. a chair or a bed ("ubiquitous"). The concept "wearable" corresponds to a device that is as unobtrusive as clothing [30]. The interest in wearable systems originates from the need to monitor patients over long periods [30]. The concept "ubiquitous", instead, refers to monitoring of the subjects under their natural physiological status [118].

The second application area of this thesis concentrates on plantar pressure mapping. Pressure mapping provides information on the interface pressure distribution between a

person and surface the person is on [26]. In medical applications, the surface is commonly a bed or a wheelchair. Also devices for plantar pressure measurements, i.e. pressure measurements between foot and ground or shoe, are developed. Depending on the magnitude and duration of the pressure, it can cause pain and tissue injuries, such as pressure ulcers, to the person. By means of pressure mapping technology, it is possible to detect the areas where the pressure has high values and thus prevent the development of pressure ulcers.

The pressure distribution is commonly measured with a commercial pressure mapping system. However, only the normal stress component of pressure is typically measured and reported [46]. The other component, shear stress, is often ignored, mainly due to the lack of validated and commercially available shear stress sensor [113]. Shear stress at the skin interface generates stresses that are additional to those of the normal stress [46] and thus, should also be considered. Pressure mapping is not yet widely used in clinical practice [17] and some improvements are still needed to utilize the technology more efficiently in clinical decision making.

1.1 Objectives of the thesis

Figure 1 illustrates the structure of the thesis. Measured variables as well as the sensor solutions are presented. The measured cardiopulmonary variables are heart rate, respiration and heart sounds. With plantar pressure mapping, both normal and shear stresses are considered.

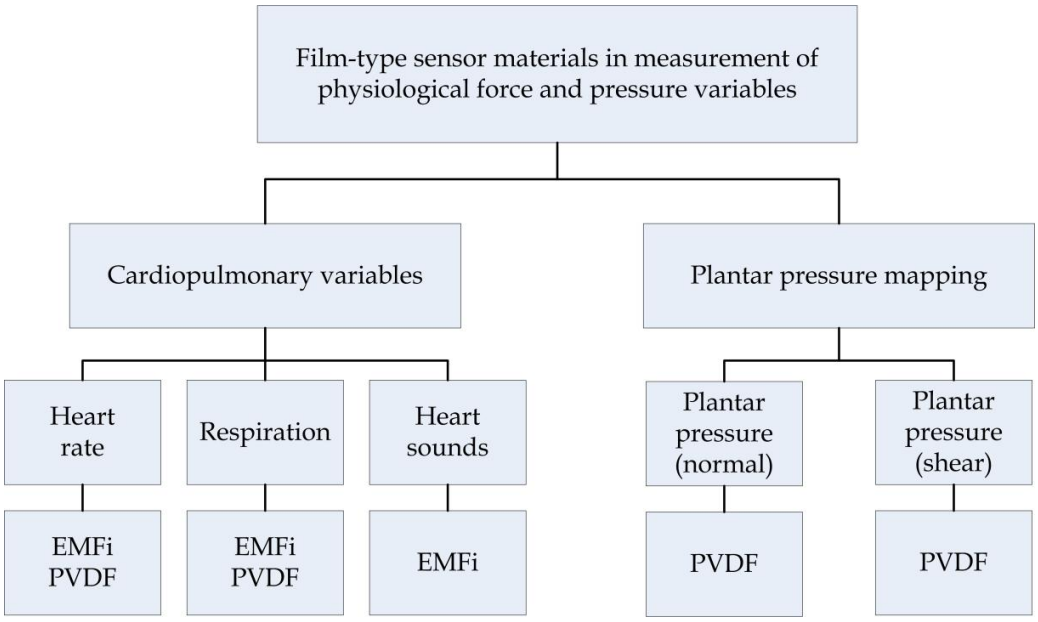

Figure 1. The structure of the thesis.

The objectives of the thesis are as follows:

- to find new, simple and inexpensive ways to measure physiological force and pressure variables needed in clinical decision making,
- to make the continuous monitoring of cardiopulmonary variables of a patient more unobtrusive and comfortable,
- to develop sensors that can be integrated into clothing or into daily life objects and thus, to minimize the sensor attachments to the patient,
- to study how to prevent pressure ulcers based on the information provided by interface pressure measurements,
- to develop a PVDF sensor prototype to measure the normal and shear stress components of the applied pressure,
- to implement a PVDF sensor with printed electrodes for normal and shear stress measurements on sole,
- to evaluate the operation of the film-type sensor materials in physiological force and pressure measurements,
- to model the sensor operation of PVDF and EMFi materials, and
- to compare the PVDF and EMFi materials.

1.2 Outline of the thesis

This thesis contains six publications and an introduction. The introduction describes the application field and briefly presents the developed measurement systems.

Publications I – V present new sensor system prototypes developed for physiological force and pressure measurements. Publication VI, instead, concentrates on the modeling of sensor operation of PVDF and EMFi materials. Also, more precise description of these materials is presented in Publication VI and the material properties are compared. Supplementary publications, Publications VII – IX, are related to the area of pressure mapping.

The introduction is organized as follows. Chapter 2 describes briefly the physiological origin of the variables measured in this thesis. Both the origins of the cardiopulmonary signals and the interface pressure are discussed. In Chapters 3 and 4, the technical backgrounds of the measurement of cardiopulmonary variables and plantar pressure mapping are presented. Chapter 5 briefly outlines the measurement systems developed. Chapter 6 summarizes the results related to Publications I – V. Chapter 7 presents the discussion and conclusions.

Chapter 2

Physiological Background

The physiological force and pressure variables discussed in this thesis are divided into two groups. The physiological origin of cardiopulmonary signals is presented in Section 2.1. In Section 2.2, the physiological background of interface pressure is introduced.

2.1 Measurement of cardiopulmonary variables

Common variables to monitor the physiological state of a patient are heart rate and respiration [19]. Body movements reflecting the physiological activity of a person are sometimes measured, too. Signals arising from these movements are usually massive and they interrupt the recognition of the other signals. Thus the heart rate and respiration are often measured at rest. To obtain more information on cardiovascular system, heart sounds can also be recorded.

The physiological origin of the heart rate, respiration and heart sounds are briefly discussed in the following subsections. Also, common methods to monitor these variables are presented. Publications I and II are related to this area (heart rate and respiration), as well as Publication III (heart sounds).

2.1.1 Heart rate

The human heart is divided into the right and left halves, each consisting of two chambers, an atrium and a ventricle [65]. The rhythmical action of the heart is controlled by an electrical signal initiated by sinoatrial (SA) node [14]. One cardiac cycle consists of two phases: the period of ventricular contraction and blood ejection, systole, and ventricular relaxation, diastole, during which the ventricle fills with blood [110]. The heart rate, the number of times the heart contracts per minute, normally varies from under 50 beats per minute in resting to over 200 beats per minute in maximal exercise [65].

The heart rate is conventionally determined by measuring electrocardiogram (ECG) with electrodes attached on the chest wall. The ECG is a record of electrical potentials generated by the heart [14]. The major electrical events of a single heartbeat are P wave, QRS complex and T wave. P wave corresponds to the atrial depolarization, QRS complex to the ventricular depolarization and T wave to the ventricular repolarization [14], [65]. The principal measurement range of the ECG is from 0.5 mV to 4 mV [114].

The origin of ballistocardiography (BCG) is in the mechanical activity of heart. However, BCG and ECG are both measuring the same event, contraction of the heart. Typically BCG lags ECG about 0.1 – 0.3 seconds [1]. The BCG signal is generated by the movement of heart and blood [51]. A sudden motion of blood mass in one direction produces recoil of body in the opposite direction [89]. The BCG is based on the measurement of this recoil with force or acceleration sensors in a sitting or supine position [89]. The typical signal range is 0-7 m*g*, where *g* is the acceleration of free fall [114]. The major motion of the body is in longitudinal direction along the axis parallel to the spine [7].

Most relevant components in the BCG signal exist within frequencies from 1 to 20 Hz [51] even though some components may also be found at frequencies up to 40 Hz [114]. Figure 2 shows a ten seconds section of (a) ECG signal and (b) BCG signal. The BCG signal is measured with a PVDF sensor on the chest wall. The main component in the BCG signal is the heart pulsation.

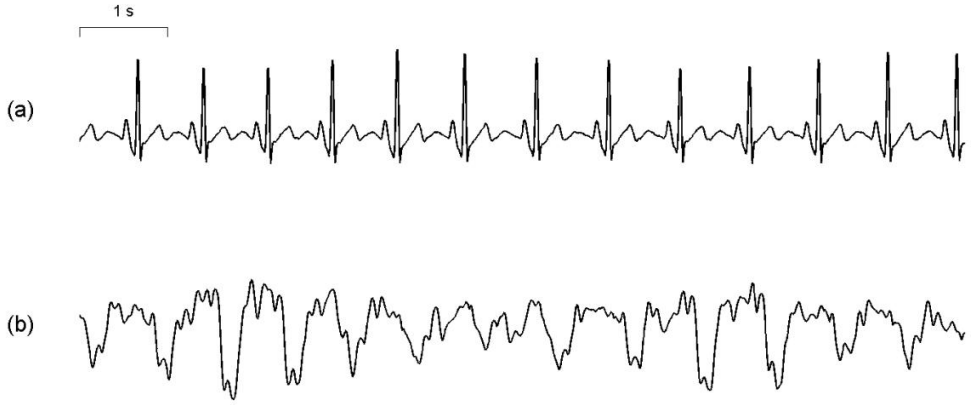

Figure 2. A section of (a) ECG and (b) BCG signals for heart rate (measured simultaneously). The BCG signal is passband filtered from 1 to 20 Hz.

The BCG waveform consists of several segments and it has different shape in contrast to the ECG signal [1]. The shape of the BCG waveform varies from one person to another and is influenced by factors such as age, body position, and respiration [7].

2.1.2 Respiration

When air is inhaled, the lungs expand and when it is exhaled, they contract [11]. The respiration involves muscles to change the volume of the thoracic cavity to generate inspiration and expiration [16]. During the flow of air into the lungs the diaphragm moves downwards and increases the lung volume [65]. Also, intercostal muscles surrounding the thoracic cavity move the rib cage in and out [16]. The breathing depends upon cyclical respiratory-muscle excitation by the motor nerves to the diaphragm and the intercostal muscles [110].

The respiration rate (RR) is the number of breaths per minute [65]. RR can vary from 2 to 50 breaths per minute [114]. RR of a normal adult is 12–15 breaths per minute [11]. Respiration rate is not completely regular and changes with exercise and during talking [11]. Common

methods to monitor the respiration rate are e.g. a strain gage positioned on chest or a nasal thermistor.

Figure 3 shows an example of respiration signals measured simultaneously with (a) a nasal NTC (negative temperature coefficient) thermistor and (b) a PVDF sensor. With the thermistor, the resistance of the element reduces as the temperature rises during the expiration [104]. The PVDF signal is measured on the chest wall.

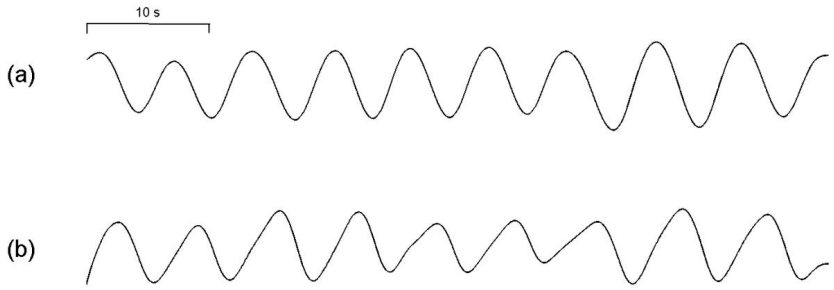

Figure 3. A section of respiration signal simultaneously measured with (a) nasal NTC thermistor and (b) PVDF sensor.

2.1.3 Heart sounds

The mechanical events in the heart give rise to the heart sounds [11]. These vibrations travel to the chest wall where they can be heard as sounds [39] through a stethoscope [11]. In phonocardiography (PCG) the sounds are recorded with a microphone [108].

The sound emitted by a human heart during a single cardiac cycle consists of two dominant events, known as the first heart sound (S1) and the second heart sound (S2) [24]. The first heart sound depicts the onset of systole, and it is produced by the closure of mitral and tricuspid valves [53]. The second heart sound is produced by the closure of the aortic and pulmonary valves, and it denotes the end of systole and the beginning of diastole [53]. S1 and S2 are always audible in a normal patient [86]. Figure 4 shows an example of typical heart sound signal measured with an EMFi sensor.

Figure 4. A period of heart sound signal. Each cardiac cycle consists of the first heart sound (S1) and the second heart sound (S2).

Additional heart sounds may occur in early diastole (the third heart sound, S3) and in late diastole (the fourth heart sound, S4). They result from rapid ventricular filling; S3 when the atrioventricular pressure gradient is high, and S4 as atrial contraction gives a boost to

ventricular filling. S3 is sometimes audible in healthy persons, but S4 is usually abnormal. [53] Besides the heart sounds, also murmurs, clicks and snaps may be heard during the cardiac cycle. Murmurs are vibrations due to the blood turbulence [114] and they may occur in normal heart or they may be caused by structural abnormalities [86]. Clicks and snaps indicate abnormality and they are associated with valve opening [86].

A lot of opinions concerning the frequency content of the heart sounds and murmurs have been presented. The first heart sound has a slightly lower frequency than the second heart sound [53]. Anand stated that the frequency range of the heart sounds is up to 100 Hz [4]. Arnott *et al*. concluded that the major concentration of energy for both the first and the second heart sounds is below 150 Hz [6]. Cameron & Skofronick [14], Carr & Brown [16] and Rushmer [89] agreed with Arnott; all stated that the frequency range of the heart sounds is from 20 to about 200 Hz. Vander *et al*. suggested a bit higher frequency range, from 40 to 500 Hz [110]. The frequencies of the murmurs are higher [124], and frequencies from 600 to 1000 Hz may exist [89]. The sound pressure level of heart sounds is rather low, from 1 Pa to 10 μPa [89].

2.2 Interface pressure

Pressure mapping provides information on the interaction between a person and the surface the person is on [26]. Depending on the magnitude and duration of the pressure, it can cause pain or tissue injuries, such as pressure ulcers, to the person. With pressure mapping technology introduced in Chapter 4, the high pressure areas can be detected and the pressure can be relieved. This section concentrates on the physiological response of interface pressure applied to human body. Especially, the origin of pressure ulcers is discussed more precisely, see Subsection 2.2.2.

2.2.1 Force and pressure

Pressure mapping is based on the basic laws of physics. A person with mass *m* being on a surface causes a force $F = mg$ to the surface. Here *g* is the acceleration of free fall. According to the Newton's third law, the surface causes an equal counterforce to the person. The forces are equal in magnitude and opposite in direction. The pressure *p* is defined as a force divided by an area $p = F/A$ and thus the force interacting with the person can be presented also as a pressure value. Although the SI-unit of pressure is pascal (Pa), millimeter of mercury (mmHg) is generally used in medical applications (1 mmHg = 0.133322 kPa). [120]

If two bodies interact by direct contact of their surfaces, normal force and friction force appear. The contact force exerted by the surface on the body can be thus presented in terms of two components of force perpendicular and parallel to surface. The perpendicular component is called as the normal force and the component parallel to surface as a friction or shear force. The result of the shear force will be a twisting or deformation of the body. Shear stress is defined as the force tangent to a material surface $F_{\parallel}$ divided by the area *A*. [120]

$$Shear\ stress = \frac{F_{\parallel}}{A} \qquad (2 - 1)$$

The level of pressure can be reduced in two ways, by redistributing the pressure away from critical to more tolerant areas or by redistributing the pressure over a larger contact area [26]. For instance, when seated, the body weight is distributed over a small surface area (ischial tuberosity) and high interface pressure is produced [22]. Instead, in supine position, the pressure is distributed over a larger surface area.

2.2.2 Pressure ulcers

Pressure ulcers, also known as pressure sores and decubitus ulcers, are a dominant health problem for people who use wheelchair or spend long period of time in bed [26]. Also, the mechanical stress between foot and shoe has a clinical relevance to various foot pathologies [46]. Abnormally high plantar interface pressures, especially with people with sensory deficits of the lower limbs, have been linked with pressure ulcers [107]. The most common cause for foot deformities and pressure ulcer formation in feet is diabetic neuropathy [83]. High pressures occur due to poor load distribution as a result of reduced sensitivity in foot [21]. At particular risk are heavily loaded regions overlying bony prominences, such as hips, heels or metatarsal heads. The metatarsus is the intermediate region of foot and consists of five metatarsal bones from medial to lateral position [109].

The pressure ulcers occur when tissue is compressed under pressure. The pressure exceeds the pressure of capillary veins, leading to the weakening of the local blood circulation and finally, to ischemic necrosis [100]. The skin of some individuals can resist much higher interface pressures than that of some others, and hence the pressure alone is not a reliable indicator of risk [92]. Pressure ulcers result from a complex set of risk factors [82] such as posture, condition of skin, incontinence and immobility [43]. However, high interface pressure related to time is believed to be the most significant factor [26]. Pressure ulcers are painful for patient [93] and increase the recovery time. Furthermore, pressure ulcers are very costly for the caregivers [93]. Plantar ulcers are difficult to heal and chronic ulceration can result in amputation of minor or major foot joint [37].

Chapter 3

Technical Background of Measurement of Cardiopulmonary Variables

In this chapter, technical background of the measurement of cardiopulmonary variables with film-type sensor materials is introduced. Section 3.1 presents the sensor materials, PVDF and EMFi, used in this thesis. In Section 3.2, the construction of the PVDF and EMFi sensors is discussed. Section 3.3 describes the measurement electronics and Section 3.4 the data collection. In Section 3.5, the data analysis methods used to explore the desired information from the signals are presented.

3.1 Film-type sensor materials

Since 1969, when a strong piezoelectric effect in polyvinylidenefluoride (PVDF) was discovered by Kawai, pyro-, piezo- and ferroelectricity have been widely investigated in a number of polar polymers, such as ferroelectric PVDF [111], [34]. The properties of these materials are related to the intrinsically anisotropic molecular structure [75]. A classical definition of piezoelectricity is the change of electrical polarization in a material in response to mechanical stress [42]. Pyroelectricity, instead, is described as production of electrical response due to the thermal excitation [35].

The studied films have usually been homogenous and solid in structure and thus the electret polymer film with cellular structure is a newcomer [77]. Non-polar cellular polymers mimic piezoelectricity by their unusual electromechanical properties [8]. Bauer *et al*. introduced a concept "ferroelectret" for these materials, since they combine features of both ferroelectrics and space-charge electrets [8]. Ferroelectricity can be described as a property of certain dielectrics that exhibit spontaneous electric polarization, that is, separation of the center of positive and negative electric charge that makes one side of the crystal positive and the opposite side negative [42]. Space-charge electrets are dielectric materials with stored quasi-permanent electrical charge [8].

There is a significant difference between cellular polymers and traditional piezoelectric polymer electrets based on polar polymers [9]. In cellular electrets the piezoelectricity is not caused by symmetry breaking on the molecular or unit cell level, but on a macroscopic level [9]. The air voids in cellular electrets serve not only to reduce the polymer's mass and hardness, but also to form macro dipoles when charged to opposite polarities on their upper

and lower internal surfaces [36]. ElectroMechanical Film (EMFi) invented in Finland in 1987 is the first truly cellular polymer electret film available for commercial applications [75].

In this thesis both film-type sensor materials are used, PVDF and EMFi. A brief introduction for the materials and also a comparison between the materials are presented in Subsections 3.1.1, 3.1.2 and 3.1.3. Subsection 3.1.4 discusses the models developed to describe the sensor operation of these materials. More detailed information on the materials and models can be found from Publication VI.

3.1.1 Polyvinylidenefluoride (PVDF)

Polyvinylidenefluoride (PVDF) is a semicrystalline polymer [74] having a solid and homogenous structure with approximately 50-65 % crystallinity [25], [84]. The chemical structure is given by $(CH_2 - CF_2)_n$ [34]. The morphology of the polymer consists of ordered regions of monomer units (crystallites) dispersed within amorphous regions [42], [123]. The atoms are covalently bonded, forming long molecular chains [111]. Because the hydrogen atoms are positively and the fluoride atoms negatively charged with respect to the carbon atoms, PVDF is inherently polar [111].

During the manufacturing process the PVDF resin pellet is brought into a sheet form with melt extrusion and the sheet is stretched [64]. Different crystal phases exist in PVDF [25], [74]: the α phase is the most stable phase at room temperature, while the β phase shows the highest piezoelectric effect [25]. Stretching at the temperature below the melting point causes a chain packaging of the molecules into parallel crystal planes, called β phase [64], [75]. These electric dipole moments are randomly oriented and result in a zero net polarization [25]. In the polarization stage, the stretched polymer is exposed to a high electric field to generate piezoelectric properties [64]. The poling procedure, in general, consists of applying an electric field for a certain period of time [35]. The molecular dipoles are oriented in the direction of the field and a net polarization is formed [25]. Finally, to provide electrodes, the film is metallized. In Figure 5, a typical charge distribution of the PVDF material is shown.

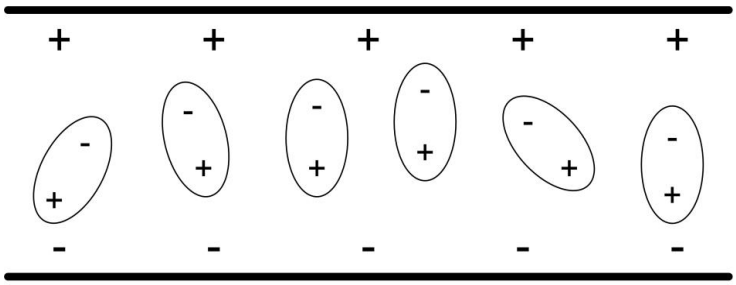

Figure 5. Simplified model structure and typical charge distribution of PVDF material [75].

If an external force compresses the film, the dipole orientation is changed and an electrical signal is induced on the electrodes [75]. This phenomenon is known as the direct effect. Piezoelectric materials also display the converse effect: mechanical deformation upon application of an electrical charge or voltage signal on the electrodes [42]. In addition, PVDF is also pyroelectric. As the film is heated, the dipoles within the film exhibit random motion

by thermal agitation, causing a reduction in the average polarization of the film and thus generating a charge build up on the film surfaces. The amount of electrical charge produced per degree of temperature increase is described by the pyroelectric charge coefficient *p*. [64]

Piezoelectricity is a cross-coupling effect between the elastic variables (stress *X* and strain *S*) and the dielectric variables (electric flux density *D* and electric field strength *E*) [35], [42]. The combinations of these variables define the four piezoelectric constants given by [35], [74]

$$d = \left(\frac{\partial D}{\partial X}\right)_E = \left(\frac{\partial S}{\partial E}\right)_X , \tag{3 - 1}$$

$$e = \left(\frac{\partial D}{\partial S}\right)_E = -\left(\frac{\partial X}{\partial E}\right)_S , \tag{3 - 2}$$

$$g = -\left(\frac{\partial E}{\partial X}\right)_D = \left(\frac{\partial S}{\partial D}\right)_X , \tag{3 - 3}$$

$$h = -\left(\frac{\partial E}{\partial S}\right)_D = -\left(\frac{\partial X}{\partial D}\right)_S . \tag{3 - 4}$$

In the equations, the first definition refers to the direct effect and the second one to the converse effect [35]. The constants are related to each other through the compliance *s* and permittivity ε [35].

$$d_{ij} = \varepsilon_0 \varepsilon_i g_{ij} \tag{3 - 5}$$

$$e_{ij} = s_{ij} d_{ij} \tag{3 - 6}$$

The piezoelectric coefficient d_{ij} possess two subscripts [64]. The coefficient is related to the electric field produced by a mechanical stress; the first subscript refers to the electrical axis and the second to the mechanical axis [64]. The d_{ij} is a third-rank tensor conventionally expressed in terms of a 3 x 6 matrix [71], [35].

$$d_{ij} = \begin{pmatrix} d_{11} & d_{12} & d_{13} & d_{14} & d_{15} & d_{16} \\ d_{21} & d_{22} & d_{23} & d_{24} & d_{25} & d_{26} \\ d_{31} & d_{32} & d_{33} & d_{34} & d_{35} & d_{36} \end{pmatrix} \tag{3 - 7}$$

The three major axes (*x*, *y* and *z*) of piezoelectric materials are referred to as 1, 2 and 3, and the shear about these axes is represented by 4, 5 and 6, respectively [85]. The axis 1 refers to the stretching direction, the axis 2 to the transverse planar direction and the axis 3 to the poling axis which is perpendicular to the material surface.

Crystal symmetry reduces the number of independent piezoelectric coefficients [71]. The symmetry class of the poled polymer is orthorhombic 2*mm* [123], for which the matrix can be written as [35]

$$d_{ij} = \begin{pmatrix} 0 & 0 & 0 & 0 & d_{15} & 0 \\ 0 & 0 & 0 & d_{24} & 0 & 0 \\ d_{31} & d_{32} & d_{33} & 0 & 0 & 0 \end{pmatrix} . \tag{3 - 8}$$

For a uniaxially-drawn sample, 1 is taken along the draw axis and it follows that $d_{31} \neq d_{32}$ and $d_{15} \neq d_{24}$ [35]. The piezoelectric coefficients d_{31}, d_{32} and d_{33} of PVDF are related with each other according to [35]

$$d_{32} = 0.1 \cdot d_{31} , \quad (3 - 9)$$

$$d_{33} = -1.5 \cdot d_{31} . \quad (3 - 10)$$

The piezoelectric coefficients of the PVDF material tend to increase with temperature [111]. The temperature dependence of the piezoelectric d_{ij} coefficient is reported e.g. in references [111], [64] and [123].

The electric flux density D and output voltage V_0 of a PVDF sensor are expressed as [64]

$$D = \frac{Q}{A} = d_{3n} X_n , \quad (3 - 11)$$

$$V_0 = g_{3n} X_n t . \quad (3 - 12)$$

In the equations, Q is the charge, A is the electrode area, d_{3n} and g_{3n} are the piezoelectric coefficients for the axis of applied stress, X_n is the applied stress and t is the film thickness. Since the electrodes are on the top and at the bottom of the film, the electrical axis is always 3. The mechanical axis n can be 1, 2 or 3 since the stress can be applied to any of these axes. [64]

The PVDF material used here was purchased from Measurement Specialties Inc. The 110 μm and 28 μm thick films with silver ink metallization and 28 μm thick unmetallized film were used. The thicker film is for applications where maximum robustness is needed.

3.1.2 ElectroMechanical Film (EMFi)

Electromechanical film (EMFi) is a thin polypropylene film having a special cellular structure. The internal cellular structure is made by stretching the polypropylene (PP) film preform during manufacturing both in longitudinal and transversal directions [54]. The film is charged by corona discharge method using electric field strength exceeding locally the film dielectric strength [78]. While charging EMFi, the corona charging produces a rather inhomogeneous surface charge in the case of local breakdown events in the foil [77]. This, however, is also been noticed to be the basis of the EMFi's effective operation [77]: when the charging electric field strength is strong enough to cause internal electrical breakdown inside the film, the sensor sensitivity starts to appear [76]. Finally, the film is metallized on both sides to provide electrodes.

The EMFi material is sensitive to dynamic forces exerted normal to its surface [77]. With cellular polymers, large values up to several hundreds pC / N are achieved for d_{33}, while the d_{31} and d_{32} coefficients are only of the order of one pC / N [9]. The pyroelectric response of EMFi is very weak [75]. The high sensitivity and low pyroelectric response of the EMFi material make it ideal for dynamic force and pressure measurements. The pyroelectricity may create problems especially in signal analysis of low frequency measurements [58].

The EMFi material consists of three layers: smooth and homogenous surface layers and a dominant, thicker midsection [57]. The midsection is full of flat, air filled voids separated by thin polypropylene layers [77]. The total thickness of the EMFi material is only a few dozens of micrometers. Figure 6 shows a SEM (scanning electron microscope) picture of the structure and Figure 7 a typical charge distribution of the EMFi material.

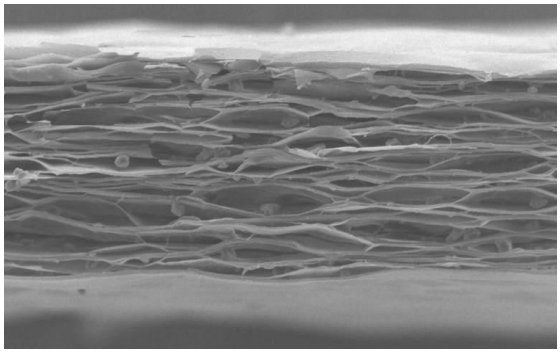

Figure 6. The structure of EMFi material. Photo: courtesy of VTT.

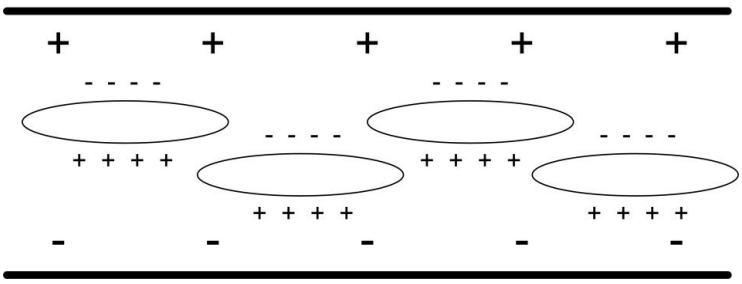

Figure 7. Simplified model structure and typical charge distribution of EMFi [75].

The sensor operation has a capacitive nature and it is based on thickness variations in the midsection of the film caused by external force [77]. The change in thickness modifies the macro dipoles and generates a corresponding charge and hence, a voltage to appear at the electrodes. When the force is applied to the EMFi material, the thickness of the polymer layers will change much less than the thickness of the air voids due to their lower stiffness. Thus the electromechanical signal of the EMFi mainly arises from the movement of the charged polymer layers with respect to the other layers and is not of piezoelectric origin. Hence the film is sometimes called as “quasi-piezoelectric” material. [29]

The output voltage ΔV of an EMFi sensor can be calculated as [28]

$$\Delta V = \left(\frac{1}{C}\right) \cdot S_q \cdot \Delta F \,, \qquad (3 - 13)$$

where ΔF is the impact force, C the capacitance and S_q the sensitivity of the sensor [28].

The stiffness of the PP material increases at lower temperature, thus decreasing the d_{33} coefficient of the film [75]. Paajanen *et al*. measured the sensor sensitivity as a function of

ambient temperature; the temperature dependence clearly changes at 278 K, which relates to the glass transition temperature of the film [76].

The EMFi material is commercially available through a Finnish company Emfit Ltd. The material used in this thesis was 70 μm thick equipped with aluminium electrodes.

3.1.3 Comparison between PVDF and EMFi materials

Table 1 lists the typical properties of a 28 μm thick PVDF material and a 70 μm thick EMFi film. Due to the structural differences, some of the material properties differ remarkably, see Table 1. For instance, differences in operation under static compression exist. The vast dynamic range of the PVDF material covers pressures from 1 μPa to 5 GPa [58]. The piezoelectric output is essentially independent on static pressure and hence, the PVDF material can be used e.g. in hydrophone applications [119]. With the EMFi material, instead, the static pressure compresses the film and reduces the thickness of the gas voids inside the film [75]. Hence, the sensitivity of the EMFi material decreases as a function of increasing static pressure [77]. The maximum pressure that can be measured by using the EMFi material is around 1 MPa [58].

Table 1. Typical properties of 28 μm thick PVDF with silver ink metallization and 70 μm thick EMFi materials [58], [64], [75], [91].

Property	Symbol	PVDF 28 μm	EMFi 70 μm	Unit
Piezoelectric coefficient	d_{33} d_{31}	$-33 \cdot 10^{-12}$ $23 \cdot 10^{-12}$	$170 \cdot 10^{-12}$ $2 \cdot 10^{-12}$	CN^{-1}
Young's modulus	Y	$2 \cdot 10^{9} - 4 \cdot 10^{9}$	$< 1 \cdot 10^{6}$	Nm^{-2}
Pyroelectric coefficient	p	$30 \cdot 10^{-6}$	$0.25 \cdot 10^{-6} - 0.45 \cdot 10^{-6}$	$Cm^{-2}K$
Capacitance	C	380	14	$pFcm^{-2}$
Permittivity	ε	$106 \cdot 10^{-12} - 113 \cdot 10^{-12}$	$10 \cdot 10^{-12}$	Fm^{-1}
Relative permittivity	$\varepsilon/\varepsilon_0$	12 – 13	1.2	-
Mass density	ρ	$1.78 \cdot 10^{3}$	330	kgm^{-3}
Dynamic range	p	$1 \cdot 10^{-6} - 5 \cdot 10^{9}$	$< 1 \cdot 10^{6}$	Pa
Temperature range	T	-40 to +80 … 100	-40 … +50	°C
Glass transition temperature	T_c	233	278	K

3.1.4 Models of sensor operation

Several approaches to model the PVDF and EMFi materials have been reported during the last decade. Lindner *at al*. developed a structural model for piezoelectricity in these materials: the model consists of negatively and positively charged particles connected by springs with different spring constants [60]. Also functional models have been reported. Brown & Carlson developed an impedance-fit method for determining the piezoelectric properties of piezoelectric polymer films (PVDF and P(VDF-TrFE)) by incorporating these properties into an electromechanical circuit model that predicts the performance of ultrasound transducers [12]. Also other similar models for PVDF have been reported, see e.g.

[32]. With the EMFi material, instead, Paajanen *et al.* proposed an elementary model with one air gap structure to describe the operation as a sensor [78]. Also a multiple air gap structure has been developed [75], [76]. Similar approaches with cellular film have been done by Hillenbrand & Sessler [45].

Piezopolymer and electret film materials behave like a capacitive generator type sensors giving an electric output signal without any external electrical excitation [58]. At the low-frequency end of the spectrum, a simple R-C model adequately describes electrical device behavior [13], see Figure 8.

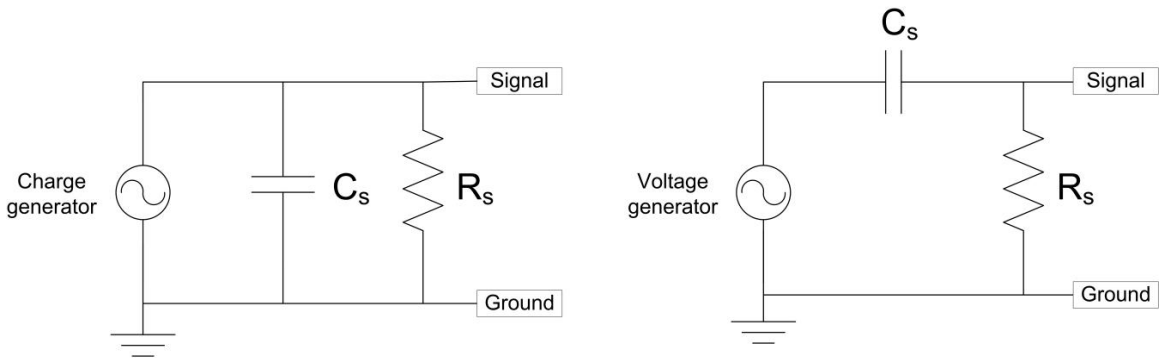

Figure 8. Equivalent circuits of PVDF and EMFi sensors.

At higher frequencies more complex models are needed [13]. A lumped-parameter equivalent circuit for a piezoelectrically excited vibrator is presented in IEEE standards [47]. The circuit parameters are assumed to be constant and independent of frequency for a narrow range of frequencies near the resonance frequency [47]. Due to the lossy nature of some polymers, the IEEE standards are not adequate, and other techniques are needed to describe piezoelectric properties more accurately [42], see e.g. reference [12].

In Publication VI, a lumped model for PVDF and EMFi sensors was developed to describe the interaction between an electrical signal and mechanical motion. The electrical energy provided by the film due to an external mechanical energy is modeled as a transformer. Transformer is used to aid in translating variables from one energy domain to another [90]. The model is described more precisely in Publication VI.

3.2 PVDF and EMFi sensors

In Publications I - V, the PVDF and EMFi sensors are implemented from commercial film materials. The film-type materials are easy to cut to almost any shape and size [77]. Ready-made sensors are also commercially available but here the sensors were chosen to be self-made. With self-made sensors more versatile sensor shapes and sizes are possible.

To construct a self-made sensor, some points should be considered, such as shielding the sensor against electromagnetic interference and moisture. The sensors implemented from the PVDF and EMFi materials are susceptible to electromagnetic interference due to the capacitive nature of the sensors [64]. To eliminate these problems, the sensors can be

shielded with a stacked sensor structure and by using a coaxial cable in data transfer. For example, if the sensor is to be mounted on a conductive substrate, the substrate may form one half of a grounded envelope with the outer electrode forming the other half [64]. Alternatively, the sensor may have a two-layer folded structure: in the folded sensor structure, the inner surface of the sensor acts as the signal electrode and the outer surface as a grounded electric shield. In addition, the PVDF and EMFi sensors can be sealed hermetically against moisture. For instance, plastic sheeting can be used.

The EMFi material used here was metallized on both sides by sputtering to provide the electrodes. The thickness of the electrodes is only a few dozens of nanometers and thus, the conductivity of the electrodes can be ensured by gluing a layer of aluminium foil on the electrodes. This also provides a better mechanical protection. To prevent short circuits, the thin aluminium metal coating is easy to remove from the material edges with a cotton stick dipped in alcohol [56]. With the PVDF material, instead, the screen printed electrodes of conductive silver ink are much thicker, about 5-10 μm [64].

The sensors constructed from the PVDF and EMFi materials are thin and lightweight. Hence, the lead attachment technique to be used to connect the wires on the sensor electrodes should have certain properties, such as low mass, low profile and high flexibility. Mechanical strength and long-term stability of the attachment technique should be considered, too. Different lead attachment techniques are available; see e.g. reference [64]. For instance, crimp-through connectors or a copper foil tape connection may be used. The copper foil tape connection method is used in the studies related to this thesis. The copper foil tape connection, however, is only a temporary method. To obtain a long-term connection, the penetrative crimp-through connector method should be used instead.

The thin sensors constructed from PVDF and EMFi materials can be integrated into various mechanical structures. Especially the EMFi material with thin electrodes is soft and flexible and it is possible to cover even round or concave surfaces [77]. When attaching the sensors constructed from PVDF and EMFi materials on a certain surface, it must be ensured that the surface is smooth and clean enough. For instance, especially in floor sensor systems, some dirt may stay between the sensor and floor and the sensor breaks down when a subject walks over the sensor. In addition, with self-made sensors, the sensor structure may not always be completely uniform, e.g. some air bubbles may remain between the sensor and the plastic sheeting during the sensor construction. Thus more reliable and sophisticated manufacturing methods to construct a sensor are still needed.

More detailed description of the sensor structures is presented in Publications I, II, III and IV. In these publications, the sensors are constructed from commercial metallized materials. In Publication V, instead, the sensor is constructed from an unmetallized PVDF material with a method of printing electrodes on the PVDF substrate.

3.3 Measurement electronics

Two basic operational amplifier circuits are generally used for the PVDF and EMFi sensors: a voltage amplifier with high input impedance or a charge amplifier that short-circuits the capacitive source [27], [58], [64].

The charge amplifier, shown in Figure 9 (a), consists of an operational amplifier with an external capacitor C_f and a resistor R. On the passband, the voltage output of the amplifier is determined by $V_{out} = Q / C_f$ [64], where Q is the charge arising in the sensor. Since the sensor is short-circuited, its capacitance does not affect [58]. Thus, with a large sensor with high capacitance, the charge generated by the sensor can be measured with a charge amplifier [58]. Also, the charge amplifier is recommended when a long cable is used between the sensor and the amplifier: the output voltage of the amplifier depends only on the feedback capacitance and thus the output voltage is independent of the cable capacitance [64].

The non-inverting voltage amplifier, shown in Figure 9 (b), consists of an operational amplifier and two external resistors, R_1 and R_2 [33]. The gain is determined as $A = 1 + R_2 / R_1$ [33]. The advantage of the voltage amplifier is a smaller sensitivity to ambient temperature: the g constant variation over temperature is smaller than the d constant variation [64].

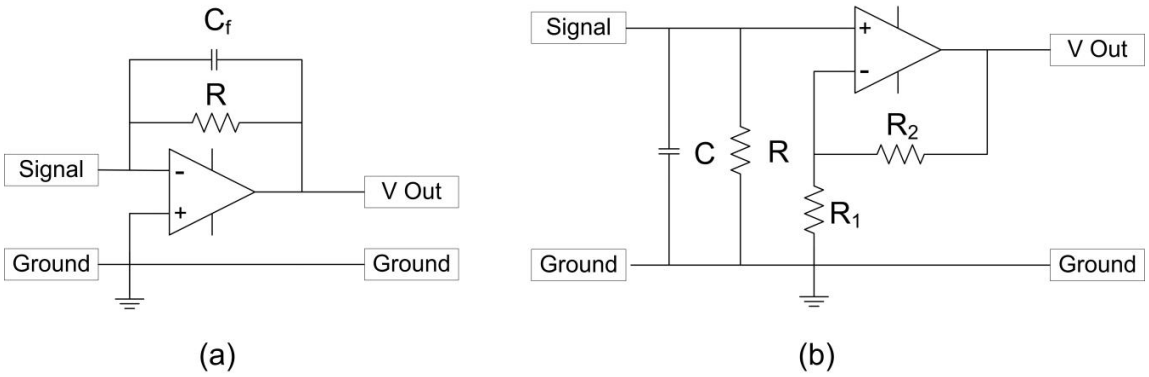

Figure 9. (a) Charge amplifier and (b) non-inverting voltage amplifier.

The low-frequency cut-off of the charge amplifier is determined by the time constant $\tau = RC_f$ [27], [64].

$$f_{low} = \frac{1}{2\pi R C_f} \quad (3 - 14)$$

With non-inverting voltage amplifier, the low-frequency cut-off is set with optional capacitor C and resistor R; if these components are not used, the cut-off frequency is formed by the input resistance of the amplifier and sensor capacitance. For a small sensor with low sensor capacitance, an amplifier with very high input impedance would be needed to keep the cut-off frequency low enough and the bandwidth wide. [58]

The noise of an operational amplifier is characterized by two noise sources: a voltage source with spectral density e_n and a current source with spectral density i_n [33]. For instance, AD820 operational amplifier (Analog Devices) is recommended by Emfit Ltd to be used in amplifier circuits [27]. The AD820 amplifier has the input voltage noise of 16 nV/$\sqrt{\text{Hz}}$ and the input current noise of 0.8 fA/$\sqrt{\text{Hz}}$ at 1 kHz [3].

Circuit simulation by computer has become a powerful tool in the analysis and design [33]. Before building the circuit, it can be simulated to find out if it works as required. A wide range of circuit simulation packages is available, although probably the best known is SPICE (Simulation Program with Integrated Circuit Emphasis) [102]. In the circuit simulations carried out here, Orcad Capture version 10.0 was used.

3.4 Data collection

During the past decade, the miniaturization and cost reduction brought by the semiconductor industry have made it possible to create computers that are small, powerful enough to carry out the processing required and affordably enough to be considered as disposable. In addition, advances in wireless communication, sensor design and energy storage technologies have made truly pervasive Wireless Sensor Networks (WSN) available. However, the WSNs are not ideally suited to monitoring the human body and its internal environment. This has led to the development of a Wireless Body Sensor Network (BSN) platform, specifically designed for the wireless networking of implantable and wearable body sensors. The BSNs offer e.g. monitoring of patients with chronic diseases, monitoring of hospital patients and monitoring of elderly patients. [118]

In this thesis, the developed systems are not wireless at the moment. To collect the data, the measurement electronics is connected to a computer by using National Instruments SCB-68 connector block. The resolution of the system, the smallest signal increment that can be detected by a measurement system [68], is 16 bits. Input voltage range ± 10 V and sampling rate 1000 Hz are used in the data collection. The data is collected and analysed with the Matlab® software. In the future, however, the systems may be designed to be wireless.

3.5 Digital signal processing

Most signals in nature are analogue in form, meaning that they vary continuously with time. The signals used in digital signal processing are typically derived from analogue signals by sampling them at regular intervals and converting them in a digital form. Digital signal processing is needed, for example, to remove interference or noise from the signal or to obtain the spectrum of the data. [48]

In this thesis, the measured signals are first filtered to reveal the desired frequency components of the signals, see Subsection 3.5.1. Power spectral density (PSD) function discussed in Subsection 3.5.2 reveals information in the frequency domain and it is used here to establish the frequency composition of the data [10].

3.5.1 Digital filtering

Common filtering objectives are to improve the quality of a signal, e.g. to remove or reduce noise, [48] or to separate the frequency components of the signal [10]. On the basis of magnitude response, filters are classified as lowpass, highpass, bandpass and bandreject filters [33]. For instance, a lowpass filter eliminates all of the signal spectral content above its

cut-off frequency [15]. More detailed information on the digital filtering design can be found e.g. from [15], [48] and [72].

With digital filtering, heart rate, respiration, and in some cases, also heart sounds can be revealed from the same signal. To filter the signals, a digital Butterworth filter is used here. Butterworth filters are defined by the property that the magnitude response is maximally flat in the passband [72]. The gain of Butterworth approximation is:

$$|H(j\omega)| = \frac{1}{\sqrt{1+\epsilon^2(\omega/\omega_c)^{2n}}} \ , \qquad (3 - 15)$$

where n is the order of the filter, ω_c is the cut-off frequency, and ϵ is a constant that determines the maximum passband variation as $A_{\max} = A(\omega_c) = 20 \cdot log_{10}\sqrt{1+\epsilon^2} = 10 \cdot log_{10}(1+\epsilon^2)$. Near ω_c a Butterworth curve rolls of at ultimate rate of $-20n$ dB/dec at the stopband. [33]

The digital filtering is utilized e.g. in Publication I to reveal heart pulsation and respiration components, see Figure 10.

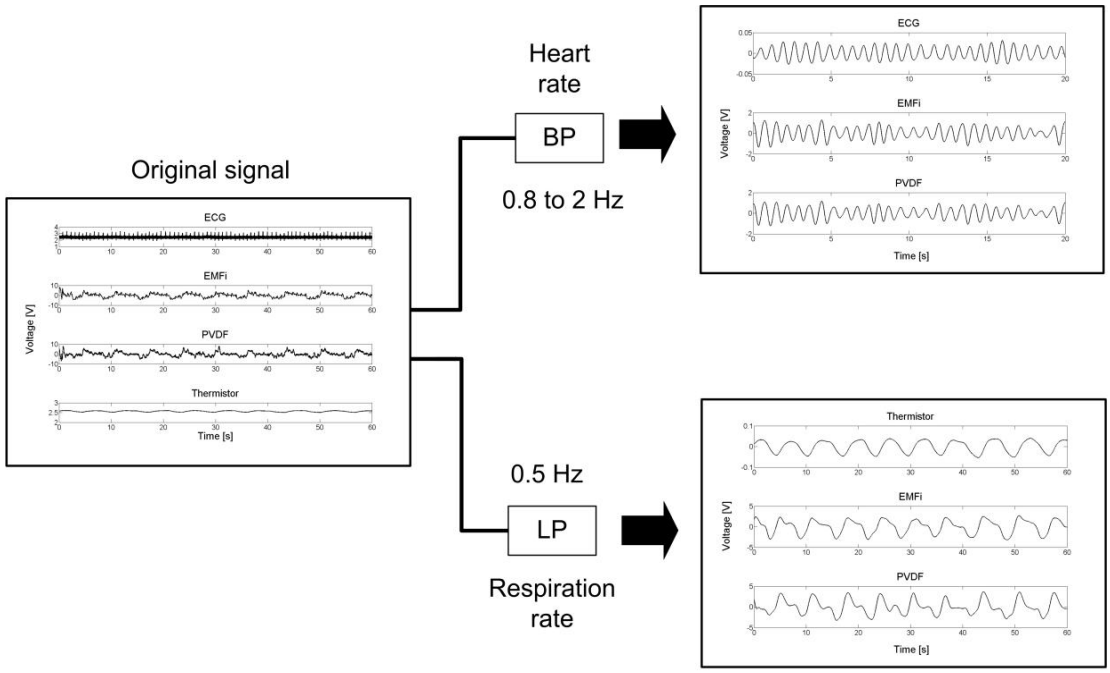

Figure 10. The original signals measured with PVDF and EMFi sensors are filtered to reveal the heart pulsation and respiration components (Butterworth second order bandpass (BP) and lowpass (LP) filters). ECG is used as a reference signal for the heart rate and a nasal thermistor for the respiration.

3.5.2 Power spectral density estimate

The power spectral density (PSD) function describes the frequency composition of the data [10]. Several methods for computation of PSD estimates are available. The Fourier transform

of the autocorrelation function is known as the correlogram method or the Blackman-Tukey estimate of PSD [50]. By directly Fourier transforming the data, we obtain the periodogram or Cooley-Tukey spectrum estimate [50].

Here the PSD estimate is calculated by using the Welch method of averaged periodograms. The method is based on the fast Fourier transform algorithm used to estimate the power spectra. The method involves sectioning the data record to segments, possibly overlapping, and taking modified periodograms of these segments. [115]

The record is divided into *K* segments $X_1(j), \ldots, X_K(j)$ with $j = 0, \ldots, L-1$ indexing the data points in each segment. For each segment of length *L* the modified periodogram is calculated by selecting a data window $W(j)$ and taking Fourier transform $A_k(n)$ for each segment $k = 1, \ldots, K$ as [115]

$$A_k(n) = \frac{1}{L}\sum_{j=0}^{L-1} X_k(j)W(j)e^{-2kijn/L} \ , \qquad (3 - 16)$$

where $i = (-1)^{1/2}$ and *n* is the index for the Fourier transform components, $n = 0, \ldots, L/2$. The overlap ratio *r* = 50 % is often preferred in PSD estimations [50]. The overlapping is needed to reduce the variance of the averaged periodogram estimate [50].

For each segment the modified periodogram is computed as [115]

$$I_k(f_n) = \frac{L}{U}|A_k(n)|^2 \ , \ k = 1, 2, \ldots, K, \qquad (3 - 17)$$

where

$$f_n = \frac{n}{L} \ , \ n = 0, \ldots, L/2 \qquad (3 - 18)$$

and

$$U = \frac{1}{L}\sum_{j=0}^{L-1} W^2(j) \ . \qquad (3 - 19)$$

U is a coefficient to remove the windowing effect from the total signal power [50], [115]. Finally, the Welch spectral estimate is the average over the periodogram estimates [115]

$$\hat{P}(f_n) = \frac{1}{K}\sum_{k=1}^{K} I_k(f_n) \ , \qquad n = 0, \ldots, L/2 \qquad (3 - 20)$$

The PSD method is used in Publications I and II to determine the average heart rate and in Publication III to find out the frequency content of heart sounds.

Chapter 4

Technical Background of Pressure Mapping

In this chapter, technical background of pressure mapping is introduced. In Section 4.1, the present state of the technology is described. Sections 4.2 and 4.3 concentrate on plantar pressure measurements, including both normal and shear stress measurements, respectively.

4.1 Pressure mapping technology

Already in 1925 the physiological responses of skin to prolonged mechanical loading were studied [31]. The development of pressure mapping systems has enhanced pressure ulcer risk assessment [23]. This is mainly due their ability to objectively measure interface pressure [23]. The risk areas can be detected with pressure mapping system and the pressure can be reduced e.g. by selecting an appropriate pressure-relieving cushion or an insole. Pressure mapping technology has become commercially available over the past decade due to the improvements in data processing and sensor technology [38] and nowadays, several systems are commercially available, see e.g. [106], [112] and [117].

Measurement of interface pressure, pressure applied to the skin by a supporting surface, provides information on the magnitude and distribution of the forces between the skin and the surface [43]. The surface can be e.g. a bed mattress, a wheelchair or a shoe. The pressure distribution is measured to find out the regions of the body where the pressure has high values to prevent the pressure ulcers (see Section 2.2). A discrete sensor or a matrix of multiple sensors can be used to measure the force acting on each sensor. The discrete sensor requires a clinician to choose the appropriate locations for optimal data collection. The use of matrix sensor enables the simultaneous measurement of a larger area usually with a constant sensor spacing. [73]

Commercial pressure mapping systems typically consist of a sensor mat, read-out electronics and computer and special software to analyse the pressure data. The sensors in the sensor pad are arranged in an array. The size of the array and the type of the sensor can vary depending on the manufacturer. Each sensor gives the magnitude of pressure as well as the location of the applied pressure [66]. Nowadays there are three generally used types of sensor technologies: resistive, capacitive and piezoresistive [38]. Pneumatic transducers have also been used [38], [94].

The pressure values measured are typically shown as a pressure map, as a colour-coded contour map [101]. The main advantage of the pressure mapping technology is thus to have an illustrative image of pressure distribution with one measurement. In addition, pressure mapping also provides quantitative data, which is not based on a subjective opinion, to support clinical findings [99]. However, there are no standard guidelines for pressure measurement and thus the sensor systems and results are difficult to compare [26]. Also, pressure mapping systems on the market are mainly designed for commercial applications. For example, they are used by the manufacturers to design, develop and test new cushions or mattresses [92].

An evaluation of commercial pressure mapping system should always be done before using the system in actual physiological measurements, as discussed in Publication VII. Size of the sensor mat, the number of sensors, and the sensitivity of the system will influence the measured pressure values [26]. Ferguson-Pell and Cardi tested the properties including hysteresis, stability, and hammocking. Hysteresis is the output's dependence to vary whether pressure is increasing or decreasing. For stability, the pressure mapping system should provide a constant output as long as constant pressure is applied. The hammocking is defined as the effect of sensor mat on the measurement; the mat tends to act as an additional cover over the cushion. [31] Hence, the sensor mat should be as thin as possible to minimize the force redistribution due to the pads themselves [93]. According to Shelton and Lott, reliability variables include creep, drift, accuracy, repeatability, and resolution. Creep is the system's tendency to vary over time when exposed to a constant pressure. Instead, drift is a system's tendency to float higher or lower values over numerous measurements. Repeatability is a system's ability to report a consistent measurement pressure every time it is used under the same conditions. Accuracy is defined as the ability to report actual pressures. [94]

The in-shoe plantar pressure measurement provides a challenging measurement environment for the sensor. Several challenges are associated with the in-shoe measurement, such as crosstalk between elements, error due to the bending forces and the difficulty of calibration [21]. High sensitivity and linearity as well as a low hysteresis of a single sensor are essential in order to ensure accurate and reliable plantar pressure recording [88]. The sensor should also be robust and have a minimal effect on the distribution of forces [85]. The sensor always measures the average pressure over the whole sensor element surface and thus, for small anatomic structures a larger sensor underestimates the real pressure values [88].

Even with the limitations of the pressure mapping technology, however, it can provide useful information on the interface pressure distribution. Several advantages can be found, e.g. the prevention of pressure ulcers [23], [43] and pressure relief of individuals with impaired sensation [92]. In addition, pressure mapping technology is often used for relative comparison between different types of cushions [92], especially with wheelchair users. In the area of plantar pressure mapping, suitable shoes or insoles can be tested. The method can also be utilized in the evaluation of surgery operation or physiotherapy by comparing the before and after pressure distributions. In addition, gait analysis is a useful tool in the design and development of prosthetic devices [88].

4.2 Plantar pressure mapping (normal stress)

Reduction of peak plantar pressure on foot during walking has become a primary focus of prevention and treatment of pressure ulcers [107]. Information about the loading of the anatomical structures of the foot is obtained especially, if the measurement is carried out without shoes [88]. In the barefoot measurement, the gait disorders can be attributed to a specific region of the foot [88].

Rahman *et al*. used a commercial Tekscan F-Scan in-shoe pressure sensor to measure the normal pressure. The sensor consists of 960 resistive sensing elements with a spatial density of 4 elements per square centimeter. The study examined the plantar pressure distribution in healthy subjects and diabetic type 2 subjects with and without neuropathy. [83] Zequera *et al*. measured the pressure distribution with a commercial Parotec pressure registration system. The Parotec system containing 24 solid state extensometric gauge type sensors is an electronic system used for measuring the pressure distribution on the plantar surface of the foot within the shoe while a subject is standing or walking. [121], [122] Other commercial devices for plantar pressure assessment are, for instance, TekScan MatScan [106] and FSA OrthoTest [112]. The MatScan system designed for barefoot plantar pressure measurement while walking or standing consists of 2288 separate sensors with an active area of 435.9 mm x 368.8 mm [106]. The FSA OrthoTest system, instead, has an active area of 350 mm x 350 mm with 1024 separate sensors [112].

Also, besides the commercial devices, a number of systems have been developed by several research groups. For instance, Morsy & Hosny developed a system for assessment of plantar pressure distribution of diabetic patients. The system includes an image acquisition subsystem composed of a standard commercial scanner and image processing subsystem. The idea relies on tissue blanching due to the applied pressure. [67] Also the EMFi material has been used: Hannula *et al*. developed an insole sensor consisting of 16 EMFi sensors. A distinct correlation between the sensor output voltage and the pressure applied on the sensor was reported. Also data of one gait was recorded and analysed. The insole sensor system, however, is not wireless, and this can be seen as a drawback. [41]

4.3 Plantar pressure mapping (shear stress)

The force applied to skin surface by a supporting surface has two components [43], pressure acting normal to the surface and shear stress acting tangential to the surface [61]. The shear force can further be divided into anterior-posterior (AP) and medial-lateral (ML) components [44]. Normal force is the force perpendicular to surface, AP force is the horizontal component in the movement direction, and ML force is the horizontal component to the transverse direction [88]. The shear stress is a vector addition of the AP and ML components [63]. Shear stress at the skin interface generates stresses that are additional to those of the normal stress [46].

Taylor divides the pressure into three components: compressive stress, shear stress and pinch stress. Pressure is the force distribution normal to the surface and it tends to compress the tissue, thus called as compressive stress. Shear stress is a force that exists if there is sliding between two surfaces. Shear stress is closely related to friction. Pinch stress, instead,

occurs when forces of different magnitude are applied to neighboring tissue and a tendency to move one plane more than another appears. Pinch stress acts perpendicular to the skin and is generated by the non-uniformity of pressure distribution. Figure 11 illustrates the three components of pressure defined by Taylor. In (a) an unloaded cube is presented, (b) shows the effect of compressive stress, (c) the effect of shear stress and (d) the effect of pinch stress. [105]

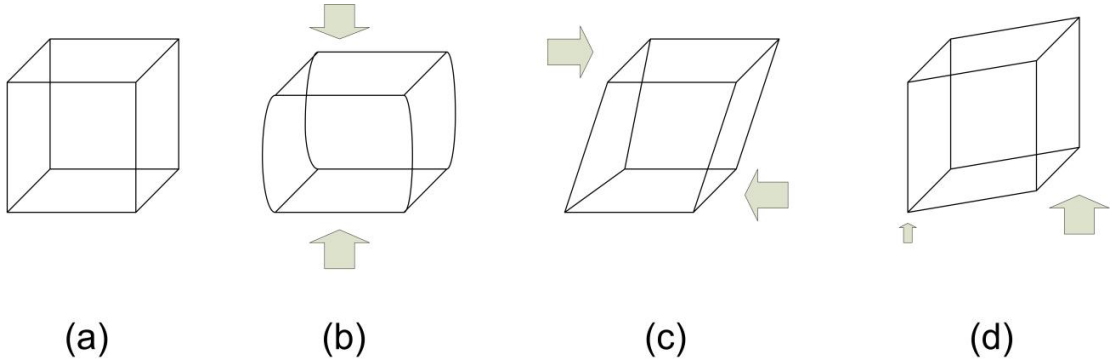

Figure 11. (a) Unloaded cube, (b) the effect of compressive stress, (c) the effect of shear stress and (d) the effect of pinch stress [105].

Typically only normal pressure is reported [46]. One of the main reasons why the shear data is not obtained is the lack of validated and commercially available shear stress sensor [113]. However, during the last decades, a variety of methods by several research groups have been developed for the measurement of shear stress. In Section 5.3 the current state of the measurement field is further discussed.

Chapter 5

Developed Measurement Systems

In this chapter, the developed measurement systems are summarized. New measurement systems are developed in Publications I - V. In addition, systems of the same kind developed by other research groups are also briefly presented.

5.1 Heart rate and respiration

New devices measuring heart rate and respiration have been developed during the last few decades. PVDF is widely used. Choi and Jiang developed a wearable cardiorespiratory sensor device for long-time monitoring [19]. The device consists of a belt sensor with PVDF film for measuring respiratory cycle and two conductive fabric sheets as heart rate electrodes. Chen *et al*. described a PVDF finger pulse and breathing wave sensor [18]. Niizeki *et al*. utilized PVDF cable sensors to detect the respiratory activity and ballistic movement due to heartbeat [70]. The cable sensors were located horizontally along the bed surface, covering the upper half of the subject's body. Siivola examined the use of PVDF to record the body movements caused by the respiration and cardiac action in lying position [96]. The PVDF elements were placed on the bed mattress. Siivola and Lang utilized PVDF wire transducers for recording of respiration at the level of the diaphragm [95]. The transducer was taped onto the abdominal skin or onto the subject's clothes.

Siivola *et al*. used electro-thermo-mechanical film (ETMF, EMFi is previously known as ETMF) in measurement of respiration [97]. The ETMF detector was placed on a bed at the level of the diaphragm. Reinvuo *et al*. developed a measurement belt equipped with accelerometers and EMFi sensor to measure respiration movements [87]. Junnila *et al*. utilized EMFi sensors installed in a chair to measure ballistocardiogram in a sitting position [1], [51], [55]. Sitting position was used since it is more natural during daily activities than the traditional supine posture [51]. Similar measurements are done by Suntila [103], Postolache *et al*. [81] and Kim *et al*. [52]. Suntila constructed a prototype of a chair equipped with EMFi sensors in order to measure pulse, breathing and other activities of a person sitting on the chair. The aim was to study human behavior in computer environment. Postolache *et al*. used EMFi in the measurement of heart and respiration rates. Sensors were taped on the seat and on the backrest of a chair. Kim *et al*. measured respiration with EMFi sensor mounted on the cushion of a wheelchair. Lim *et al*. used EMFi sensor attached to the back of a chair to measure mechanocardiogram on the subject's back [59]. The mechanocardiogram, a record of pressure variation on a subject's skin, was applied in the

measurement of pre-ejection period, the latency between the Q-wave and the opening of aortic valve. Alametsä *et al*. detected spiking events caused by the increased respiratory resistance from BCG data recorded with EMFi sheet [2]. Spiking is a phenomenon where BCG wave complexes increase in amplitude during increased respiratory resistance. In addition, some devices are already available commercially. For example, Emfit Ltd has developed a bed monitoring system for dementia care and epileptic seizure alarms containing an EMFi sheet sensor to be installed in a bed [29].

In Publications I and II, the PVDF and EMFi materials were used in the measurement of heart rate. In Publication I the heart rate was measured on the chest wall. The sensors were enclosed inside a textile pocket and the pocket was integrated into clothing, beneath a commercial heart rate belt (Polar). In Publication II, instead, the heart rate of a person sitting on a chair or lying in a bed was measured with sensor located beneath the legs of chair and bed. To minimize the effect of moving artifacts, the measurements were carried out at rest. In Publication I, also the measurement of respiration rate is discussed.

Similar sensors were used in Publications I and II to convert the mechanical movements provided by the pulsation of heart and respiration into electrical signals. In Publication I the sensors have a shape of rectangle with equal areas of 3 cm x 10 cm. In Publication II the developed sensor consists of separate PVDF and EMFi transducers having a shape of rectangle with equal areas (5 cm x 6.5 cm). A two-stage amplifier consisting of charge and voltage amplifiers (see Section 3.3) was used to amplify the measured signals. The charge amplifier in the first stage converts the transducer charge flow to a voltage; the voltage signal is further amplified at the second stage with a non-inverting voltage amplifier [33]. In the data analysis, the signals were filtered to separate the heart pulsation components from the measured signals (see Section 3.5.1). The average heart rate was calculated with the Welch method of averaged periodograms, as discussed in Section 3.5.2

The operation of the measurement systems presented in Publications I and II were evaluated with test measurements. In Publication I, ten measurements with PVDF and EMFi sensors were done with a subject. In Publication II, test measurements with subjects (5 male and 5 female) in sitting and supine positions were carried out. Also, the sensor operation in longer-term measurements was tested with two subjects. ECG was used as a reference signal for the heart rate. In Publication I, a nasal NTC thermistor was used as reference sensor for the respiration rate. More detailed information on the test measurements can be found from Publications I and II, respectively.

5.2 Heart sounds

Various techniques to measure the heart sounds have been reported. Most of these systems are based on the phonocardiography. The PCG signal is measured, for example, by using a digital stethoscope [40], a microphone [4] or a piezoelectric polymer film polyvinylidenefluoride, PVDF [125]. The portable fetal heart rate monitor developed by Zucherwar *et al*. consists of a PVDF sensor array mounted on a belt worn by the mother [125]. Also Ansourian *et al*. utilized PVDF to measure foetal breathing movement and foetal heart sounds by monitoring maternal abdominal wall movements [5].

Publication III introduces a measurement system for the heart sounds implemented with EMFi material. The mechanical vibrations caused by the cardiac structure were converted into an electrical signal by the EMFi transducer. The transducer has a two-layer folded structure with shape of a rectangle and size 7 cm x 5 cm. To measure the heart sound signal, the transducer was attached on the chest wall with double-sided tape. The transducer area corresponds to the pulmonary area (below the collar bone at the left side of sternum). Digital second-order Butterworth bandpass filter with passband from 20 to 499 Hz was used to reveal the heart sounds. In addition, the 50 Hz noise was removed with an elliptic bandstop filter. The frequency content of heart sounds was computed with the Welch method of averaged periodograms, discussed in Subsection 3.5.2.

5.3 Shear force

In Publication IV, a PVDF sensor for plantar normal and shear stress measurements is introduced. The sensor simultaneously measures the normal stress and the anterior-posterior (AP) and medial-lateral (ML) components of shear stress. In Publication V the sensor was further developed: a method of printing electrodes on the unmetallized PVDF material was tested to construct a matrix version of the sensor.

5.3.1 Shear force sensor

A variety of methods to measure the shear stress are reported elsewhere. Lord and Hosein measured the shear stress locally beneath the metatarsal heads and heel [61]. The motion under the action of shear stress was detected in two orthogonal directions by magneto-resistive elements [46]. Also in-shoe plantar pressure was measured with Tekscan F-Scan Gait Analysis System. The same methodology was employed in normals [46] and patients with diabetic neuropathy [61].

Perry *et al.* recorded the forefoot shear stress and pressure during the initiation of a gait [80]. They measured simultaneously all the three components of shear stress and pressure. The system consists of 16 transducers based on strain gauge technology, each with surface area measuring 2.5 cm x 2.5 cm. Heywood *et al*. utilized capacitive technology to measure anterior-posterior and medial-lateral components of shear stress. The shear stress sensor consists of a central post and four parallel plates forming a capacitor between each face of the post and the parallel plate that it opposes. When a subject walks over the post, the forces on the plantar surface of the foot cause the post to be deflected and thus the capacitance to be altered. A commercial miniature pressure sensor was also used to measure normal pressure. [44]

Mackey & Davis developed a 16 element sensor array to measure 3D stress [63]. The system has an optical basis. Wang *et al*. developed a sensor consisting of an array of optical fibers lying in perpendicular rows and columns separated by elastomeric pads [113]. The measurement of normal and shear stresses is based on intensity attenuation in fibers due to the physical deformation of two adjacent perpendicular fibers.

Pedotti *et al*. utilized a 200 μm thick PVDF film poled in selected areas [79]. Sixteen circular disks, each with diameter of 6 mm, were deposited onto a film by vacuum evaporation to

provide the electrodes for pressure sensors. Razian & Pepper developed an in-shoe triaxial pressure transducer utilizing piezoelectric copolymer with a mixed composition of PVDF and trifluoroethylene (TrFE) [85].

The developed sensor of size 3 cm x 3 cm presented in Publication IV consists of four individual sensor elements constructed from commercial PVDF material with silver ink electrodes. The construction and structure of the sensor as well as the sensor operation principle are discussed more precisely in Publication IV. Briefly, one of the four sensor elements acts as a reference sensor on which the outputs of the other elements are compared to. Three difference signals corresponding to the signals of normal pressure and the AP and ML components of shear stress are obtained. The charge flow of sensor element was measured with a charge amplifier (AD711, Analog Devices).

Figure 12 illustrates the formation of the stress components. Direction 1 corresponds to the AP shear stress, direction 2 to the ML shear stress and direction 3 to the normal pressure. The AP shear stress is obtained as a difference signal between the sensor elements 1 and 2. The two sensor elements are placed one upon the other so that the force components in directions 2 and 3 are eliminated. The ML shear stress and normal stress are correspondingly obtained. The ML shear stress is the difference signal between the sensor elements 1 and 3 and the normal stress the difference signal between the sensor elements 1 and 4.

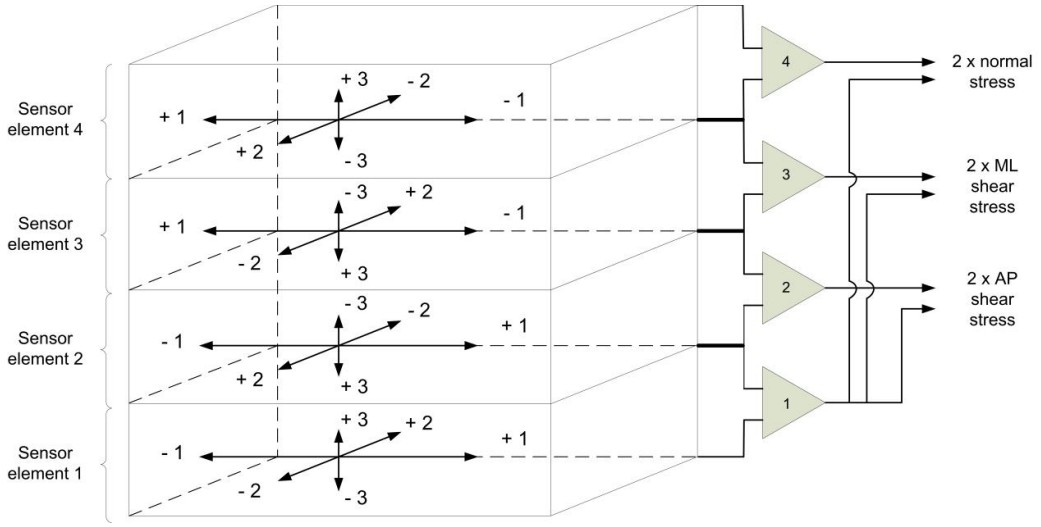

Figure 12. The normal stress (direction 3) and AP (direction 1) and ML (direction 2) shear stresses are obtained as difference signals between the sensor elements.

To convert the voltage signals provided by the sensor elements to force signals, the force sensitivities of the elements were measured. The force sensitivity in V/N was measured for each mechanical axis with Bruel & Kjaer Mini-Shaker and dynamic and static reference force sensors. The procedure of measuring the sensitivities is described more thoroughly in Publication IV.

5.3.2 Sensor with printed electrodes

In Publication V, the shear force sensor introduced in Publication IV was further developed. A method to print electrodes on the unmetallized PVDF material was tested to construct a matrix version of the sensor.

Use of the printing technologies is an additive process and it has some advantages when compared with subtractive processing methods, e.g. the number of process steps is decreased and hence, the manufacturing process is simplified. The etching process contains several stages (e.g. mask creation, resist placement, exposing and cleaning); in additive process, these steps are replaced with material jetting and sintering. Nano-sized silver particle ink was used here to form electrodes with inkjet technology. The sintering profile used was 150 °C with a period of one hour.

Figure 13 shows a schematic diagram of the PVDF sensor with printed electrodes. In the prototype, there are 3 cm x 3 cm electrodes printed on both sides of the PVDF foil. The pads, size 5 mm x 5 mm, are needed for connecting the sensor with printed electrodes to the sensor signal amplifier. Similar amplifier was used as in Publication IV.

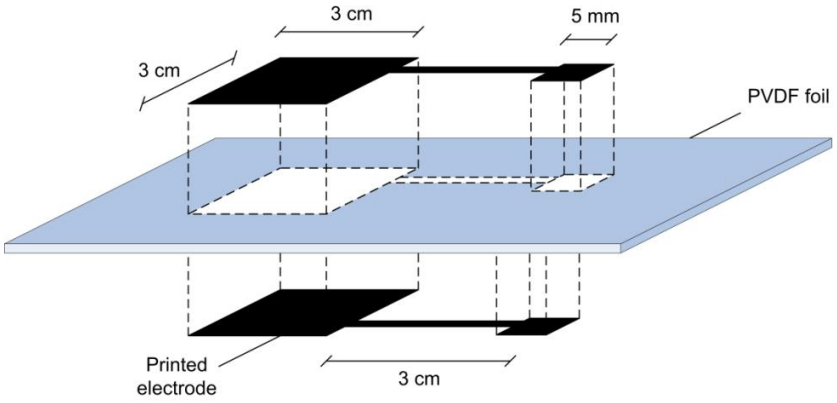

Figure 13. Schematic of the PVDF sensor with printed electrodes.

The thermal stress caused by the printing process may affect the PVDF material properties, and thus, the study presented in Publication V was concentrated on the characteristics of single sensors manufactured with this method. The operation of the PVDF sensor with printed electrodes was evaluated with similar sensitivity measurements as carried out in Publication IV and the results were compared.

Chapter 6

Summary of Results

In this chapter, the results are summarized. Section 6.1 is related to the systems of cardiopulmonary signals (Publications I - III) while Section 6.2 concentrates on the pressure mapping technology (Publications IV - V). Publication VI, instead, is more general, and the results of the publication are not discussed in this section.

6.1 Cardiopulmonary signals

The following subsections present the results obtained in Publications I, II and III. More detailed results are found from these publications.

6.1.1 Heart rate and respiration

In Publication I, the aim was to study whether the PVDF and EMFi materials are capable to measure the heart and respiration rates correctly and also to find out the possible differences between the results. The heart rates calculated from the BCG signals measured with the PVDF and EMFi sensors mainly corresponded to the values calculated from the reference ECG signal. Some differences, however, appeared due to the different origins of the signals. The origin of BCG signal is in mechanical activity of the heart whereas the ECG describes electrical action. Similar difference between ECG and BCG signals has been previously reported by Jansen *et al*. [49]. They measured the BCG with a static charge sensitive bed (SCSB) and concluded that the difference may be due to myoclonic activity and large body movements. Since the BCG sensor measures also other mechanical movements than only the heart contraction, the BCG and ECG sensors may not provide the same heart rate value. Here the measurements were done at rest to minimize effect of movement artifacts. Differences between the heart rates obtained with the PVDF and EMFi sensors were not found. Also the respiration rates were found to be similar as the values computed from the reference thermistor signal.

In Publication II the heart rate was measured in the sitting and supine positions with the PVDF and EMFi sensors located beneath the legs of a chair and a bed. The purpose of the study was to find out if this kind of measurement is possible with the PVDF and EMFi materials. Also the differences between the results provided by the materials were investigated. The heart rates computed from the BCG signals measured with the sensors mainly corresponded to the values calculated from the reference ECG signal. Similar error

sources were found as in Publication I. However, also some differences between the results of the PVDF and EMFi sensors appeared, especially in supine position. As discussed in Chapter 2, the major forces caused by the blood flow in the vessels are directed cranio-caudally [55], along the axis parallel to the spine [7]. The BCG signal is the recoil of this blood flow and it has the opposite direction. In the sitting position, the force is exerted normal to the sensor surface and thus the PVDF and EMFi sensors should provide similar signals. This mainly occurred; the results obtained in the measurements of the sitting position were rather similar as the results of Publication I. However, some differences may still appear, e.g. the sitting position in the chair may affect the results. In the supine position, instead, the force is not perpendicular to the sensor surface. Hence, stress may be applied also to the directions of the mechanical axes 1 and 2 of the PVDF material. The measurements carried out in Publication II thus suggest that the material sensitivities to different force directions may affect the results especially in the measurements of the supine position.

In Publications I and II, the PSD method used in the data analysis provides an average heart rate. The average heart rate can also be deduced by studying the autocorrelation of the measured signal. The autocorrelation function describes the general dependence of the values of the data at one time on the values at another time [10]. Autocorrelation can then reveal information about the periodicity of the studied signal. To evaluate the sensor operation in real-time detection of heart rate, more sophisticated analysis methods are needed. For instance, Akhbardeh *et al*. has developed a heart disease diagnosing system clustering the BCG cycles from the signal measured with an EMFi sensor installed under the upholstery of a chair [1].

The measurement systems developed in Publications I and II are useful especially in measurements where exact heart rate values are not needed. Application areas can be found e.g. from home care. In addition, the advantage of the system presented in Publication II is insensitivity to temperature; the sensor is not in contact with the patient and thus the body temperature does not affect the results. The systems reported in Publication I and II also make the continuous monitoring of cardiopulmonary variables of a patient more unobtrusive and comfortable. No sensor attachments are needed, since sensors can be integrated into clothing or daily life objects such as chair or bed. Hence, several advantages can be found when comparing the developed systems with present-day systems (e.g. ECG).

To conclude, both the PVDF and EMFi materials seem to be suitable for these kinds of measurements of heart and respiration rates. However, to further evaluate the sensors, more test measurements are still needed, especially with persons having different body morphologies. Also, the effect of movement artifacts should be considered more thoroughly.

6.1.2 Heart sounds

The results of Publication III proved that EMFi is a suitable material for the measurement of heart sounds. The frequency content of the heart sounds concentrated on the frequencies up to 80 Hz, corresponding to the results reported by the others, see Section 2.1.3.

The developed measurement system for the heart sounds has certain advantages. When compared to conventional microphones, the extraneous noises coupled via air do not easily

disturb the measurement: the EMFi transducer attached on the chest wall is sensitive to mechanical vibrations only. In addition, the operation is more straightforward than in conventional stethoscopes, where a bell is required as an impedance matcher between the air and skin [14]. Some disadvantages, however, also appeared. Due to the low pressure level of the heart sounds, the background interference might be a problem. Hence, shielding the sensor against electromagnetic interference should especially be considered.

As well as the heart sounds, also the heart and respiration rates can be determined from the signals measured with the transducer at rest. Hence, with the EMFi material and by using more sophisticated methods to manufacture the transducer, it would be possible to implement a plaster-like transducer measuring vital signals.

6.2 Pressure mapping

The following subsections present the results obtained in Publications IV and V. More detailed results are found from these publications.

6.2.1 Shear force sensor

The aim of Publication IV was to develop a normal and shear stress sensor measuring the plantar stress during gait. The PVDF material was chosen since it is capable to measure the forces also in the directions of mechanical axes 1 and 2.

The average force sensitivities computed from the calibration results were (12.6 ± 0.8) mV / N for the normal force, (223.9 ± 20.3) mV / N for the AP shear force and (55.2 ± 11.9) mV / N for the ML shear force. The values are presented as mean sensitivities ± standard deviations. Also some preliminary plantar pressure measurements with the developed sensor were done. The average normal peak-to-peak pressure of the five consecutive steps in the hallux was (98.9 ± 23.4) kPa, in the medial metatarsal heads (164.3 ± 43.9) kPa, in the lateral metatarsal heads (142.5 ± 9.1) kPa and in the heel (157.3 ± 32.5) kPa. The corresponding average peak-to-peak shear stress in the hallux was (33.0 ± 1.8) kPa, in the medial metatarsal heads (49.8 ± 3.7) kPa, in the lateral metatarsal heads (43.7 ± 2.0) kPa and in the heel (48.6 ± 9.9) kPa. The results are mainly comparable with the results reported by others, see e.g. [46], [62], [80]. However, the plantar pressure measurement carried out here has certain limitations. For instance, the sensitivities of the separate sensor elements were not exactly the same and thus some errors in the plantar pressure signals may appear.

Despite of the promising results obtained in this study, the developed sensor is a preliminary prototype. Further development is still needed. At the moment, the sensor is rather large and capable to discrete measurements only. With more sophisticated manufacturing methods smaller sensors in matrix could be produced. The goal is to further develop the sensor structure and to design a matrix sensor to be used in in-sole measurements of plantar pressure distribution.

6.2.2 Sensor with printed electrodes

The results of Publication V indicate that the method of printing electrodes on the unmetallized PVDF material reduce the sensor sensitivity. The main reason for the decreased sensitivity is the thermal stress caused by the printing process: the sintering temperature of 150 °C used in the study is close to the melting point of the PVDF material (around 175 °C at 0 MPa [25]). Due to the large thermal stress, the PVDF was contracted. The shrinkage was estimated to be around 15 % in stretching direction (axis 1). In perpendicular planar direction (axis 2), instead, the shrinkage was not noticed.

Average sensitivities computed from the data of sensors were (2.8 ± 0.9) mV/N for the normal force, (23.0 ± 6.6) mV/N for the AP shear force and (4.7 ± 1.5) mV/N for the ML shear force. Hence, in the normal force direction the sensor sensitivity was found to be about fifth and in shear force directions about tenth of the corresponding values measured with the sensor manufactured from the metal-coated material.

However, despite the descent in sensitivity values, the sensor sensitivity is still adequate for plantar pressure measurements. Hence, the method to print electrodes on the unmetallized PVDF material seems to be suitable to construct a matrix sensor for normal and shear stress measurements on sole. In order to improve the sensitivity of the developed stress sensor, the thermal stress of the PVDF material must be lower, and thus, the temperature of the sintering phase must be decreased in future. The options to decrease the thermal stress are to use nanoparticles that have lower sintering temperature or use advanced sintering methods such as a laser, electrical sintering or pulse sintering. In addition, there might be a way to recover the original sensitivity of the PVDF material by a poling step after electrode printing process.

Chapter 7

Discussion and Conclusions

Flexible and thin sensor materials are useful especially in physiological applications where the sensor is in contact with skin [77]. The sensor can be integrated into clothing or into daily life objects (e.g. a chair or a bed), and the electrode attachments to patient can be minimized. The use of the measurement system is aimed to be as unobtrusive and comfortable for the users as possible. In Publications I, II and III, such measurement systems were developed and presented.

Based on the results obtained in Publications I and II, PVDF and EMFi are appropriate materials for the measurements of the heart and respiration rates. Both materials are sensitive to dynamic forces only, and thus they are useful especially in this kind of measurements of physiological pulsatile signals. Both materials generate a charge when they are mechanically deformed and thus, in principle, operate similarly. Due to the structural differences between the materials, however, some of the material properties differ remarkably; the semicrystalline PVDF material has homogenous and solid structure whereas the structure of the EMFi material is cellular. For instance, it should be noted that the materials are sensitive to different force directions: the d_{33} of the PVDF material and S_q of the EMFi material has the same direction while PVDF recognizes also the forces in the directions of the mechanical axes 1 and 2. If only uniaxial pressure is studied, the property to produce signals from mechanical excitation originating from multiple directions may be a problem [75]. If the stress is applied to more than one mechanical axis simultaneously, the output voltage is formed by the stress components on these axes.

The measurement system for the heart sounds presented in Publication III provided promising results. In future applications, a plaster-like transducer utilizing film-type sensor materials could be implemented to measure vital signals. Heart sounds as well as heart and respiration rates could be measured with the sensor. Due to the low base material cost, disposable sensors could also be used [77]. Application areas can be found e.g. from home care.

The advantage of the EMFi material over other polymer electrets is based on its flexibility due to the voided internal structure [77]. The base material of EMFi is inexpensive PP, which makes it applicable also for large area sensors like floor monitoring systems [58], [77]. In Publication VI, the sensitivity of the EMFi material in thickness direction was found to be approximately five-fold ((58.7 ± 16.5) mV / N) when compared to the corresponding value of the PVDF material ((12.6 ± 0.8) mV / N). The higher sensitivity of the EMFi material is mainly

due to the internal voided structure. However, due to the relatively large gas voids and local corona breakdowns, sensitivity varies in different parts of the film [98]. When compared to the EMFi material, piezoelectric polymers usually contain fluoride which is a potentially toxic substance; this can be considered as a disadvantage [75], [58]. The main advantage of the PVDF material, however, is its sensitivity to forces related to its length and width. This property creates many versatile applications for the material, e.g. the material can be utilized also as a shear stress sensor.

Typically, commercial pressure mapping systems measure only the normal stress, while the effect of the shear stress is neglected. The shear stress at the skin interface generates stresses which are additional to those of the normal stress [46] and hence, should also be considered. The shear stress sensor developed in Publications IV and V offer a possibility to measure the AP and ML components of the shear stress as well as the normal stress simultaneously. Some of the systems previously reported utilize separate normal and shear stress sensors [46], [44]. The comparison of data obtained from two different systems is not possible due to the different sensor technologies [85] and thus the capability to measure all the three force components with a single sensor is a useful property. Such a system is not available commercially at the moment. Several application areas can be found, e.g. plantar pressure measurements or measurement of the normal and shear stresses in the operation tables in long lasting operations and in intensive care. Paralyzed patients are also in need of sensitive sensors in their cushions and mattresses especially if they already have suffered from pressure ulcers. Besides the medical applications, a lot of other application areas are available for the pressure sensor capable to measure the normal and shear stresses, such as sport or industrial applications. However, the operating temperature of the PVDF material may limit the possible application areas.

To conclude, despite the promising results obtained in this thesis, more research is still needed to examine the material properties before the PVDF and EMFi sensors can be used in large scale commercial applications. For instance, the effect of moisture and ageing should be studied more thoroughly before integrating the sensors in physiological applications. In addition, more reliable and sophisticated manufacturing methods to construct a sensor or a sensor matrix are still needed.

Bibliography

[1] A. Akhbardeh, S. Junnila, M. Koivuluoma, T. Koivistoinen, V. Turjanmaa, T. Kööbi & A. Värri. Towards a heart disease diagnosing system based on force sensitive chair's measurement, biorthogonal wavelets and neural networks. *Engineering Applications of Artificial Intelligence*, Vol. 20, p. 493-502, June 2007.

[2] J. Alametsä, E. Rauhala, E. Huupponen, A. Saastamoinen, A. Värri, A. Joutsen, J. Hasan & S.-L. Himanen. Automatic detection of spiking events in EMFi sheet during sleep. *Medical Engineering & Physics*, Vol. 28, p. 267-275, April 2006.

[3] Analog Devices, AD820 Single-Supply, Rail-to-Rail, Low Power, FET Input Op Amp datasheet. Available online at: http: / / www.analog.com (accessed 7 October 2008).

[4] R.S. Anand. PC based monitoring of human heart sounds. *Computers and Electrical Engineering*, Vol. 31, p. 166-173, March 2005.

[5] M.N. Ansourian, J.H. Dripps, J.R. Jordan, G.J. Beattie & K. Boddy. A transducer for detecting foetal breathing movements using PVDF film. *Physiological Measurement*, Vol. 14, p. 365-372, Aug. 1993.

[6] P. Arnott, G. Pfeiffer & M. Tavel. Spectral analysis of heart sounds: relationships between some physical characteristics and frequency spectra of first and second heart sounds in normals and hypertensives. *Journal of Biomedical Engineering*, Vol. 6, p. 121-128, April 1984.

[7] L.C. Barna. Acquisition systems and analysis methods for human originated signals. Doctoral Thesis, Tampere University of Technology, 2008.

[8] S. Bauer, S. Bauer-Gogonea, M. Dansachmuller, I. Graz, H. Leonhartsberger, H. Salhofer & R. Schwodiauer. Modern electrets. *IEEE Symposium on Ultrasonics*, p. 370-376, Oct. 2003.

[9] S. Bauer, S. Bauer-Gogonea, M. Dansachmuller, H. Hoislbauer, M. Lindner & R. Schwodiauer. Physics of electromechanically active, cellular materials. *11th Int. Symposium on Electrets*, p. 50-53, Oct. 2002.

[10] J.S. Bendat & A.G. Piersol. Random data: Analysis and measurement procedures. John Wiley & Sons, New York, 1971.

[11] B.H. Brown & R.H. Smallwood. Medical physics and physiological measurement. Blackwell Scientific Publications, London, 1981.

[12] L.F. Brown & D.L. Carlson. Ultrasound transducer models for piezoelectric polymer films. *IEEE Trans. Ultrasonics, Ferroelectrics and Frequency Control*, Vol. 36, p. 313-318, May 1989.

[13] R.H. Brown. Piezo film: Form and function. *Sensors & Actuators A: Physical*, Vol. 22, p. 729-733, June 1989.

[14] J. Cameron & J. Skofronick. Medical physics. Wiley & Sons, New York, 1978.

[15] J.V. Candy. Signal processing. The modern approach. McGraw-Hill Book Co., Singapore, 1988.

[16] J.J. Carr & J.M. Brown. Introduction to biomedical equipment technology. John Wiley & Sons, New York, 1981.

[17] P.R. Cavanagh, B.A. Lipsky, A.W. Bradbury & G. Botek. Treatment for diabetic foot ulcers. *The Lancet*, Vol. 366, p. 1725-1735, Nov. 2005.

[18] Y. Chen, L. Wang & W.H. Ko. A piezopolymer finger pulse and breathing wave sensor. *Sensors and Actuators A: Physical*, Vol. 23, p. 879-882, April 1990.

[19] S. Choi & Z. Jiang. A novel wearable sensor device with conductive fabric and PVDF film for monitoring cardiorespiratory signals. *Sensors and Actuators A: Physical*, Vol. 128, p. 317-326, April 2006.

[20] S. Choi & Z. Jiang. A wearable cardiorespiratory sensor system for analyzing the sleep condition. *Expert Systems with Applications*, Vol. 35, p. 317-329, July-Aug. 2008.

[21] J. Cobb & D.J. Claremont. Transducers for foot pressure measurement: survey of recent developments. *Medical and Biological Engineering and Computing*, Vol. 33, p. 525-532, July 1995.

[22] S.A. Crawford, M.D. Stinson, D.M. Walsh & A.P. Porter-Armstrong. Impact of sitting time on seat-interface pressure and on pressure mapping with multiple sclerosis patients. *Archives of Physical Medicine and Rehabilitation*, Vol. 86, p. 1221-1225, June 2005.

[23] S.A. Crawford, B. Strain, B. Gregg, D.M. Walsh & A.P. Porter-Armstrong. An investigation of the impact of the Force Sensing Array pressure mapping system on the clinical judgement of occupational therapists. *Clinical Rehabilitation*, Vol. 19, p. 224-231, March 2005.

[24] S.M. Debbal & F. Bereksi-Reguig. Time-frequency analysis of the first and the second heartbeat sounds. *Applied Mathematics and Computation*, Vol. 184, p. 1041-1052, Jan. 2007.

[25] G. Eberle, H. Schmidt & W. Eisenmenger. Piezoelectric polymer electrets. *IEEE Trans. Dielectrics and Electrical Insulation*, Vol. 3, p. 624-646, Oct. 1996.

[26] I. Eitzen. Pressure mapping in seating: a frequency analysis approach. *Archives of Physical Medicine and Rehabilitation*, Vol. 85, p. 1136-1140, July 2004.

[27] Emfit Ltd. Basic preamplifiers for Emfit Sensors. 2003. Available online at: http://www.emfit.com (accessed 7 October 2008).

[28] Emfit Ltd. Calculating the output voltage of Emfit sensors. 2003. Available online at: http://www.emfit.com (accessed 7 October 2008).

[29] Emfit Ltd. Homepage of Emfit Ltd. Available online at: http://www.emfit.com (accessed 7 October 2008).

[30] M. Engin, A. Demirel, E.Z. Engin & M. Fedakar. Recent developments and trends in biomedical sensors. *Measurement*, Vol. 37, p. 173-188, March 2005.

[31] M. Ferguson-Pell & M. Cardi. Pressure Mapping Systems. *TeamRehab Report*, p. 28-32, Oct. 1992.

[32] A.S. Fiorillo. Noise analysis in air-coupled PVDF ultrasonic sensors. *IEEE Trans. Ultrasonics, Ferroelectrics and Frequency Control*, Vol. 47, p. 1432-1437, Nov. 2000.

[33] S. Franco. Design with operational amplifiers and analog integrated circuits. McGraw-Hill, New York, 2002.

[34] E. Fukada. History and recent progress in piezoelectric polymers. *IEEE Trans. Ultrasonics, Ferroelectrics and Frequency Control*, Vol. 47, p. 1277 – 1290, Nov. 2000.

[35] T. Furukawa. Piezoelectricity and pyroelectricity in polymers. *IEEE Trans. Electrical Insulation*, Vol. 24, p. 375-394, June 1989.

[36] R. Gerhard-Multhaupt. Less can be more. Holes in polymers lead to a new paradigm of piezoelectric materials for electret transducers. *IEEE Trans. Dielectrics and Electrical Insulation*, Vol. 9, p. 850-859, Oct. 2002.

[37] C. Giacomozzi & F. Martelli. Peak pressure curve: An effective parameter for early detection of foot functional impairments in diabetic patients. *Gait & Posture*, Vol. 23, p. 464-470, June 2006.

[38] R.J. Goldman & R. Salcido. More than one way to measure a wound. *Advances in Skin & Wound Care*, Vol. 15, p. 236-243, Sept./Oct. 2002.

[39] A. Guyton. Textbook of medical physiology. W.B. Sounders, Philadelphia, 1976.

[40] L.T. Hall, J.L. Maple, J. Agzarian & D. Abbott. Sensor system for heart sound biomonitor. *Microelectronics Journal*, Vol. 31, p. 583- 592, July 2000.

[41] M. Hannula, A. Säkkinen & A. Kylmänen. Development of EMFI-sensor based pressure sensitive insole for gait analysis. *IEEE Int. Workshop on Medical Measurement and Applications*, 2007.

[42] J.S. Harrison & Z. Ounaies. Polymers, Piezoelectric. Encyclopedia of Smart Materials. John Wiley & Sons, Inc., 2002.

[43] C. Harstall. Interface pressure measurement systems for management of pressure sores. *Alberta Heritage Foundation for Medical Research*, Sept. 1996.

[44] E.J. Heywood, D.C. Jeutter & G.F. Harris. Tri-axial plantar pressure sensor: design, calibration and characterization. *26th Annual Int. Conf. IEEE Engineering in Medicine and Biology Society*, p. 2010 – 2013, 2004.

[45] J. Hillenbrand & G.M. Sessler. Piezoelectricity in cellular electret films. *IEEE Trans. Dielectrics and Electrical Insulation*, Vol. 7, p. 537-542, Aug. 2000.

[46] R. Hosein & M. Lord. A study of in-shoe plantar shear in normals. *Clinical Biomechanics*, vol. 15, p. 46-53, Jan. 2000.

[47] IEEE Standard on Piezoelectricity (IEEE Standard 176-1987), Institute of Electrical and Electronic Engineers, NY, 1988.

[48] E.C. Ifeachor & B.W. Jervis. Digital signal processing: A practical approach. Addison-Wesley Publishers Ltd., Wokingham, 1993.

[49] B. Jansen, B. Larson & K. Shankar. Monitoring of the ballistocardiogram with the static charge sensitive bed. *IEEE Transactions on Biomedical Engineering*, Vol. 38, p. 748-751, Aug. 1991.

[50] H. Jokinen. Analysis of non-stationary measurement signals: Aspects of preprocessing and spectrum estimation. Doctoral Thesis, Tampere University of Technology, 2003.

[51] S. Junnila, A. Akhbardeh, A. Värri & T. Koivistoinen. An EMFi-film sensor based ballistocardiographic chair: performance and cycle extraction method. *IEEE Workshop on Signal Processing Systems Design and Implementation*, p. 373-377, 2005.

[52] J.-M. Kim, J.-H. Hong, M.-C. Cho, E.-J. Cha & T.-S. Lee. Wireless biomedical signal monitoring device on wheelchair using noncontact Electro-mechanical Film sensor. *29th Annual Int. Conf. IEEE Engineering in Medicine and Biology Society*, p. 574-577, 2007.

[53] B. Kirby & K. MacLeod. Clinical examination of the heart. *Medicine*, Vol. 34, p. 123-128, April 2006.

[54] K. Kirjavainen. Electromechanical Film and procedure for manufacturing same. U.S. Patent No. 4654546, 1987.

[55] T. Koivistoinen, S. Junnila, A. Värri & T. Koobi. A new method for measuring the ballistocardiogram using EMFi sensors in a normal chair. *26th Annual Int. Conf. IEEE Engineering in Medicine and Biology Society*, p. 2026-2029, 2004.

[56] S. Kärki, T. Salpavaara & J. Lekkala. EMFi in wearable audio applications. *4th International Workshop on Wearable and Implantable Body Sensor Networks*, p. 86-91, 2007.

[57] J. Lekkala & M. Paajanen. EMFi - New electret material for sensors and actuators. *10th Int. Symposium on Electrets*, 1999, p. 743-746, Sept. 1999.

[58] J. Lekkala, J. Tuppurainen & M. Paajanen. Material and operational properties of large-area membrane type sensors for smart environments. *XVII IMEKO World Congress*, 2003.

[59] Y.G. Lim, K.H. Hong, K.K. Kim, J.H. Shin & K.S. Park. Mechanocardiogram measured at the back of subjects sitting in a chair as a non-intrusive pre-ejection period measurement. *Pervasive Health Conference and Workshops*, p. 1-4, Nov. -Dec. 2006.

[60] M. Lindner, H. Hoislbauer, R. Schwodiauer, S. Bauer-Gogonea & S. Bauer. Charged cellular polymers with "ferroelectretic" behavior. *IEEE Trans. Dielectrics and Electrical Insulation*, Vol. 11, p. 255-263, Apr. 2004.

[61] M. Lord & R. Hosein. A study of in-shoe plantar shear in patients with diabetic neuropathy. *Clinical Biomechanics*, Vol. 15, p. 278-283, May 2000.

[62] D.J. Lott, D. Zou & M.J. Mueller. Pressure gradient and subsurface shear stress on the neuropathic forefoot. *Clinical Biomechanics*, Vol. 23, p. 342-348, March 2008.

[63] J.R. Mackey & B.L. Davis. Simultaneous shear and pressure sensor array for assessing pressure and shear at foot / ground interface. *Journal of Biomechanics*, Vol. 39, p. 2893-2897, 2006.

[64] Measurement Specialties Inc. Piezo film sensors. Technical manual. 86 pages. Available online at: http: / / www.meas-spec.com (accessed 2 July 2007).

[65] D. Moffett, S. Moffett & C. Schauf. Human physiology. Wm. C. Brown Publishers, Dubuque, Iowa, 1993.

[66] L. Mohanty, S.C. Tjin & N.Q. Ngo. Pressure mapping sensor with an array of chirped sampled fiber gratings. *Sensors and Actuators A: Physical*, Vol. 117, p. 217-221, Jan. 2005.

[67] A.A. Morsy & A. Hosny. A new system for the assessment of diabetic foot planter pressure. *26th Annual Int. Conf. Engineering in Medicine and Biology Society*, p. 1376-1379, 2004.

[68] National Instruments. DAQ SCB-68 68-Pin Shielded Connector Block User Manual, 2002. Available online at: http: / / www.ni.com (accessed 7 October 2008).

[69] F. Nebeker. Golden accomplishments in biomedical engineering. *Engineering in Medicine and Biology Magazine*, Vol. 21, p. 17-47, May-June 2002.

[70] K. Niizeki, I. Nishidate, K. Uchida & M. Kuwahara. Unconstrained cardiorespiratory and body movement monitoring system for home care. *Medical and Biological Engineering and Computing*, Vol. 43, Nov. 2005.

[71] J. F. Nye. Physical properties of crystals. Oxford University Press, London, 1969.

[72] A.V. Oppenheim & R.W. Schafer. Digital Signal Processing. Prentice-Hall Inc., New Jersey, 1975.

[73] M.N. Orlin & T.G. McPoil. Plantar Pressure Assessment. *Physical therapy*, Vol. 80, p. 399-409, April 2000.

[74] Y. Osada & D.E. DeRossi. Polymer sensors and actuators. Springer-Verlag, 2000.

[75] M. Paajanen. The cellular polypropylene electret material – Electromechanical properties. Doctoral thesis, VTT Chemical Technology, 2001.

[76] M. Paajanen, J. Lekkala & H. Välimäki. Electromechanical modeling and properties of the electret film EMFi. *IEEE Trans. Dielectrics and Electrical Insulation*, Vol. 8, p. 629-636, Aug. 2001.

[77] M. Paajanen, J. Lekkala & K. Kirjavainen. ElectroMechanical Film (EMFi) — a new multipurpose electret material. *Sensors and Actuators A: Physical*, Vol. 84, p. 95-102, Aug. 2000.

[78] M. Paajanen, H. Välimäki & J. Lekkala. Modelling the electromechanical film (EMFi). *Journal of Electrostatics*, Vol. 48, p. 193-204, March 2000.

[79] A. Pedotti, R. Assente, G. Fusi, D. De Rossi, P. Dario & C. Domenici. Multisensor piezoelectric polymer insole for pedobarography. *Ferroelectrics*, Vol. 60, p. 163-174, Oct. 1984.

[80] J.E. Perry, J.O. Hall & B.L. Davis. Simultaneous measurement of plantar pressure and shear forces in diabetic individuals. *Gait and Posture*, Vol. 15, p. 101-107, 2002.

[81] O. Postolache, P. Silva Girao, G. Postolache & M. Pereira. Vital Signs Monitoring System Based on EMFi Sensors and Wavelet Analysis. *Instrumentation and Measurement Technology Conf.*, 2007.

[82] R. Ragan, T.W. Kernozek, M. Bidar & J.W. Matheson. Seat-interface pressures on various thicknesses of foam wheelchair cushions: A finite modeling approach. *Archives of Physical Medicine and Rehabilitation*, Vol. 83, p. 872-875, June 2002.

[83] M.A. Rahman, Z. Aziz, U.R. Acharya, T.P. Ha, N. Kannathal, E.Y.K. Ng, C. Law, T. Subramaniam, W.Y. Shuen & S.C. Fang. Analysis of plantar pressure in diabetic type 2 subjects with and without neuropathy. *ITBM-RBM*, Vol. 27, p. 46-55, May 2006.

[84] N.P. Rao, J. Dargahi, M. Kahrizi & S. Prasad. Design and fabrication of a microtactile sensor. *Canadian Conf. Electrical and Computer Engineering*, p. 1167-1170, May 2003.

[85] M.A. Razian & M.G. Pepper. Design, development, and characteristics of an in-shoe triaxial pressure measurement transducer utilizing a single element of piezoelectric copolymer film. *IEEE Trans. Neural Systems and Rehabilitation Engineering*, Vol. 11, Sept. 2003.

[86] T. Reed, N. Reed & P. Fritzson. Heart sound analysis for symptom detection and computer aided diagnosis. *Simulation Modelling Practice and Theory*, Vol. 12, p. 129-146, May 2004.

[87] T. Reinvuo, M. Hannula, H. Sorvoja, E. Alasaarela & R. Myllylä. Measurement of respiratory rate with high-resolution accelerometer and emfit pressure sensor. *IEEE Sensors Applications Symposium*, p. 192-195, 2006.

[88] D. Rosenbaum & H.-P. Becker. Plantar pressure distribution measurements. Technical background and clinical applications. *Foot and Ankle Surgery*, Vol. 3, p. 1-14, 1997.

[89] R. Rushmer. Cardiovascular dynamics. 4th edition, W.B. Sounders, Philadelphia, 1976.

[90] S.D. Senturia. Microsystem design. Kluwer Academic Publishers, Boston, 2001.

[91] G.M. Sessler. Piezoelectricity on polyvinylidenefluoride. *Journal of the Acoustical Society of America*, Vol. 70, p. 1596-1608, 1981.

[92] N. Shapcott & B. Levy. By the numbers: Making the case for clinical use of pressure measurement mat technology to prevent the development of pressure ulcers. *TeamRehab Report*, p. 16-18, 20-21, Jan. 1999.

[93] F. Shelton, R. Barnett & E. Meyer. Full-body interface pressure testing as a method for performance evaluation of clinical support surfaces. *Applied Ergonomics*, Vol. 29, p. 491-497, Dec. 1998.

[94] F. Shelton & J.W. Lott. Conducting and interpreting interface pressure evaluations of clinical support surfaces. *Geriatric Nursing*, Vol. 24, p. 222-227, July-Aug. 2003.

[95] J. Siivola & A.H. Lang. Non-invasive piezoelectric transducer for recording of at the level of diaphragm. *Electroencephalography and Clinical Neurophysiology*, Vol. 106, p. 552-553, June 1998.

[96] J. Siivola. New noninvasive piezoelectric transducer for recording of respiration, heart rate and body movements. *Medical and Biological Engineering and Computing*, Vol. 27, p. 423-424, July 1989.

[97] J. Siivola, K. Leinonen & L. Räisänen. ETMF-polymer transducer as a detector of respiration in humans. *Medical and Biological Engineering and Computing*, Vol. 31, Nov. 1993.

[98] H. Sorvoja, V.M. Kokko, R. Myllylä & J. Miettinen. Use of EMFi as a Blood pressure pulse transducer. *IEEE Transactions on Instrumentation and Measurement*, Vol. 54, p. 2505-2512, Dec 2005.

[99] J. Sparacio. Pressure mapping: Potential benefits from technology. *Rehab Central Articles*, Feb. 2002.

[100] M. Stinson, A. Porter-Armstrong & P. Eakin. Seat-interface pressure: A pilot study of the relationship to gender, body mass index, and seating position. *Archives of Physical Medicine and Rehabilitation*, Vol. 83, p. 405-409, March 2003.

[101] M.D. Stinson, A.P. Porter-Armstrong & P.A. Eakin. Pressure Mapping Systems: Reliability of Pressure Map Interpretation", *Clinical Rehabilitation*, Vol. 17, p. 504-511, Aug. 2003.

[102] N. Storey. Electronics: A systems approach. Addison-Wesley Longman Ltd., Harlow, 1998.

[103] J. Suntila. Chair with EMFi sensors for physiological measurements. Master of Science thesis, Tampere University of Technology, 2004 (in Finnish).

[104] P.H. Sydenham (ed.). Handbook of measurement science. Vol. 2, Practical fundamentals. John Wiley & Sons, Chichester, 1983.

[105] G. Taylor. Pressure and shear – definitions, relationships and measurements. Vista Medical. Available online at: http://www.pressuremapping.com/File/ShearTerms.pdf (accessed 7 October 2008).

[106] Tekscan, Inc. Available online at: http://www.tekscan.com/ (accessed 12 June 2009).

[107] E. Titianova, P. Mateev & I. Tarkka. Footprint analysis of gait using a pressure sensor system. *Journal of Electromyography and Kinesiology*, Vol. 14, p. 275-281, April 2004.

[108] L. Torres-Pereira, P. Ruivo, C. Torres-Pereira & C. Couto. A noninvasive telemetric heart rate monitoring system based on phonocardiography. *IEEE Int. Symposium on Industrial Electronics*, p. 856-859, 1997.

[109] G. Tortora & S.R. Grabowski. Principles of anatomy & physiology. John Wiley & Sons, New York, 2003.

[110] A. Vander, J. Sherman & D. Luciano. Human physiology: the mechanisms of body function. 5th edition, McGraw-Hill, New York, 1990.

[111] A. Vinogradov. Piezoelectricity in Polymers. Encyclopedia of Smart Materials. John Wiley & Sons, Inc., 2002.

[112] Vista Medical Ltd. Available online at: http://www.pressuremapping.com/ (accessed 12 June 2009).

[113] W.-C. Wang, W.R. Ledoux, B.J. Sangeorzan & P.G. Reinhall. A shear and plantar pressure sensor based on fibre-optic bend loss. *Journal of Rehabilitation Research & Development*, Vol. 42, p. 315-326, 2005.

[114] J. Webster (ed.). Medical instrumentation: application and design. Houghton Mifflin, Boston, 1978.

[115] P. Welch. The use of fast Fourier transform for the estimation of power spectra: A method based on time averaging over short, modified periodograms. *IEEE Trans. Audio and Electroacoustics*, Vol. 15, p. 70-73, June 1967.

[116] WordNet®, a lexical database for English language. Available online at: http://wordnet.princeton.edu/ (accessed 12 June 2009).

[117] XSENSOR Technology Corporation. Available online at: http://www.xsensor.com/ (accessed 12 June 2009).

[118] G.-Z. Yang (ed.). Body Sensor Networks. Springer-Verlag, New York, 2006.

[119] Y. Yiquan, S. Binwen & L. Zongjie. A new multilayer planar PVDF standard hydrophone and its applications. *IEEE Trans. Ultrasonics, Ferroelectrics and Frequency Control*, Vol. 42, p. 958-964, 1995.

[120] D. Young & R. Freedman. University physics. Addison-Wesley Publishing Company, 1996.

[121] M. Zequera, S. Stephan & J. Paul. The "PAROTEC" Foot Pressure Measurement System and its Calibration Procedures. *28th Annual Int. Conf. IEEE Engineering in Medicine and Biology Society*, p. 4135-4139, 2006.

[122] M.L. Zequera, S.E. Solomonidis, F. Vega & L.M. Rondon. Study of the plantar pressure distribution on the sole of the foot of normal and diabetic subjects in the early stages by using a hydrocell pressure sensor. *25th Annual Int. Conf. IEEE Engineering in Medicine and Biology Society*, p. 1874-1877, 2003.

[123] Q.M. Zhang, V. Bharti & G. Kavarnos. Poly(Vinylidene Fluoride) (PVDF) and its Copolymers. Encyclopedia of Smart Materials. John Wiley & Sons, Inc., 2002.

[124] Z. Zhidong, Z. Zhijin & C. Yuquan. Time-frequency analysis of heart sound based on HHT. *Int. Conf. Communications, Circuits and Systems*, 2005.

[125] A. Zucherwar, R. Pretlow, J. Stoughton & D. Baker. Development of a piezopolymer pressure sensor for a portable fetal heart rate monitor. *IEEE Trans. Biomedical Engineering*, Vol. 40, p. 963-969, Sept. 1993.

Publications